FULFILLMENT OF SELECTION CRITERIA BY WITA CONCEPT OF KIT

DRAFT OF SEPTEMBER 2, 2010

	EDMS Ref:	Date: 2010-09-02
	Name	**Affiliation**
Author	A. Class, U. Fischer, S. Gordeev, R. Stieglitz, M. Majerle, P. Vladimirov	Karlsruhe Institute of Technology (KIT)
Reviewer		
Approver		

Table of Contents

1 Introduction 3

2 Concept description 3

3 Neutronics 10

3.1 Generic analyses 11

3.2 Evaluation of neutron and proton induced dpa and gas production cross-section data for Fe, Cr, Ni up to 2.5 GeV 14

3.3 Dedicated analyses for the WITA target design 16

4 Material issues 23

4.1.1 Operation conditions 23

5 Criteria evaluation 31

5.1 Criteria associated with Performance during operation 31

5.1.1 Neutron performance - Time Integrated flux instruments (SANS) 34

5.1.2 Number of possible beam lines 34

5.2 Criteria associated with Safety 34

5.2.1 Ease of containment implementation 40

5.2.2 Environmental impact beyond design basis accidents 40

5.2.3 Ease of licensing approval 40

5.3 Criteria based on Associated Risks 40

5.3.1 The need for R&D 40

5.4 Criteria based on Availability 40

5.4.1 Lifetime of TMR 40

5.5 Criteria based on Maintainability 40

5.5.1 Time required to perform maintenance/service 40

5.5.2 Ease of TMR exchange 40

5.6 Criteria based on Upgradability 40

5.6.1 Possibility to increase performance of existing system 40

6 Summary 40

1 Introduction

The European Spallation Source ESS aims at producing high energy spallation neutrons. These are produced when a high energy (W=2500 MeV) proton beam with a mean current of I=2 mA hits an appropriate target material. Besides the target material all structure materials are also subjected to the proton or neutron radiation and therefore are activated. Once the target was operational it must be remote handled in hot cells.

Inherently coupled to the desired spallation reaction is the high heat deposition in the target. This power is mainly due to the proton current and can be calculated as the product of the energy of a single electron times the number of protons per second in the beam, i.e. Q=U*I= $2.5*10^{9}$ V *$2*10^{-3}$A=5 MW.

In ESS the high beam power is provided by a pulsed source with long pulses and a repetitions rate of f=20 Hz. The deposited heat sums up to $Q_{average}$= 5 MW or Wpulse=Qaverage/f=250kJ. With each pulse the target material is heated within a few nanoseconds by an average temperature increase of deltaT which is calculated as Wpulse~m*cp*deltaT. Here m is the mass of the heated target material. The heating is non-uniform, as the heat deposition strongly varies, i.e. it exponentially decreases with the penetration depth of the beam into the target material. The maximum heat deposition is for the selected beam energy near the free surface and becomes quiet low (less than 2 orders of magnitude relative to the maximum) at a penetration depth of about 600 mm. Heating is accompanied with thermal expansion of the target material and thus with thermal stresses and potentially with pressure waves propagating through the target material.

2 Concept description

Modular Windowless Target (WITA) design:

In a windowless target the target material is a liquid metal which is pumped through a cooling cycle to remove the heat. The proton beam is directed on a free surface, so that no solid structures are subjected to the proton beam. Since the proton beam in principle can interact with any material the beam must be guided trough a vacuum environment before hitting the target. Thus, in a windowless target a free surface separates vacuum and the liquid metal target material. This free surface makes any windowless target concept an open system. In order to prevent activated target materials to enter the accelerator the target region is encapsulated in a containment using a safety window for the beam. Since the windowless target is inherently an open system the proposed modular target concept takes advantage of the open construction and allows for improved maintenance.

The WITA design is shown in figure 2.1 and consists of a pool and 3 modules and a containment (not shown in the figure):

Pump

Heat exchanger

Target

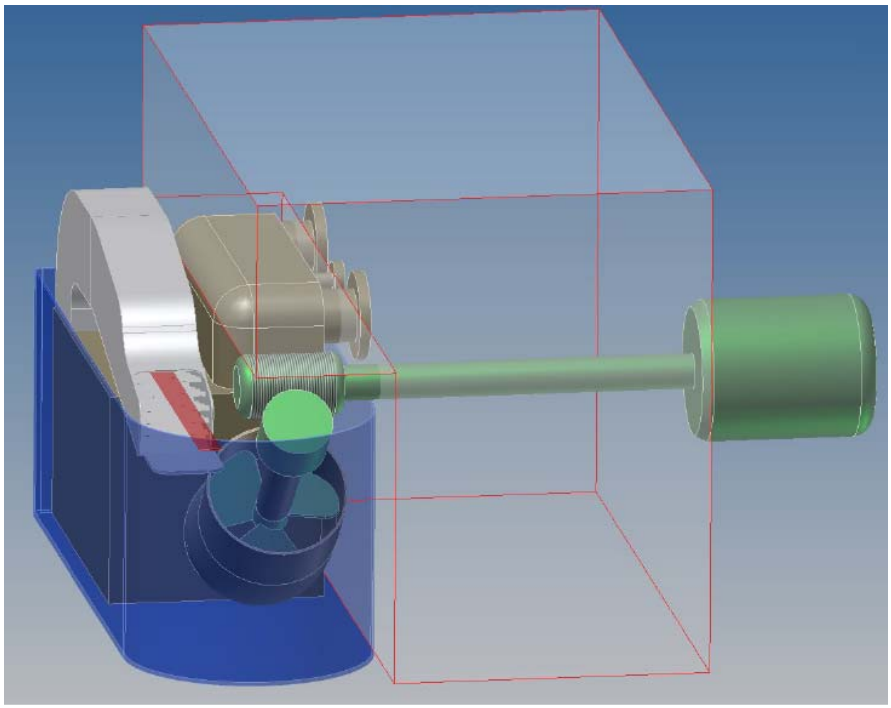

Figure 2.1: WITA target consisting of pool, pump module, heatexchanger module, and target module.

Pool

The pool contains the liquid metal which is lead bismuth eutectic in the WITA-design. LBE reaches the liquidus temperature at about 100°C. Once the target goes operational the LBE is electrically molten in the pool and will permanently stay in the liquid state. LBE expands during solidification so that freezing requires special care. By permanent heating to temperature above the liquidus temperature potential unacceptable stresses are omitted.

The inventory of LBE is the major mass of the whole target. The pool is dimensioned such that potential future upgrades of the target can be realized without the necessity to replace the activated LBE. Even though in phase I of ESS only a short 50 days lifetime of the target is required the pool is designed to withstand a much longer period of operation. The pool vessel is equipped with a number of bayonet-fixings where the modules can be attached. These bayonets are designed such that they can tolerate material swelling due to irradiation. The side walls of the pool are sufficiently high that splashing of liquid metal from the pool is suppressed. In the front wall of the pool vessel a channel is installed which represents the beam guide. This channel is sufficiently long and equipped with a drainage, ensuring secure enclosure of LBE thus preventing migration of LBE.

Pump

The coolant flow is established by an impeller pump. The impeller is submerged in the pool. The housing of the impeller is part of the pump module which is pushed into the heat exchanger module at the low pressure side. The motor axis is tilted relative to the impeller axis where a set of gears transfers the motors momentum to the impeller. Liquid metal lubrication bearings fix the axis. The motor is also a separate module. The connection of the motor axis to the gear block of the pump module is above the LBE-free surface.

Heat exchanger module

The heat exchanger must remove the heating of the beam which is nominal 5 MW. Heat transfer on the liquid metal side is very efficient due to the very high heat conductivity of liquid metals. In WITA a spray cooling on the secondary side is foreseen due to the high heat transfer, where 1MW/m^2 heat transfer area is a practical value, which can be realized with water spray cooling. Alternatively, oil can be used as the secondary fluid as realized in the MEGAPIE target. The helical pin heat exchangers employed in MEGAPIE can be installed in ESS where the higher power is obtained by increasing the number of cooling pins.

Target module

The interaction region of the proton beam with the LBE-target material is within the target module. The target module must provide optimal thermohydraulic conditions in the interaction region. In a windowless target the target module must also establish a stable free surface flow. In WITA the target module is installed at the exit of the heat exchanger. The flow is pumped upwards, then directed into a horizontal channel and then accelerated by a nozzle into an open channel which is inclined relative to the horizontal plane by a 15 degree angle. The proton beam enters the liquid metal through the free surface. Due to the inclination of the flow direction relative to the horizontal beam the required depth of the channel is approximately ¼ of the considered energy deposition length (.6m) of the beam, i.e. ¼*.6m=.15m. The small inclination angle allows having almost coaxial beam and flow as in many earlier target designs MYRRHA, MEGAPIE, EURISOL where the coolant is heated quiet uniform, so that a minimal coolant flow rate can be established. On the other hand, due to the inclination the flow component perpendicular to the beam transports the fluid across the beam in a short time. This is advantageous for pulsed beams, as successive beam pulses interact with fluid that was not subjected to the beam previously. The proposed angle of 15 degrees results in a cross velocity which is still ¼ the axial velocity. In order to ensure that no fluid is subjected multiple times to appreciable heat deposition by successive pulses, it suffices to use a maximum axial velocity of $u_{max}=4*s_{beam}*f\sim4*.02*20=1.6$m/s. Here $s_{beam}\sim.2$m is the vertical height of the beam with appreciable energy deposition.

Following each pulse a shockwave is generated due to thermal expansion. Dispersion of the shockwave is enhanced by obstacles installed in the flow channel. The dispersion of the shock wave can be further enhanced if a small amount of cover gas is entrained into the liquid metal.

In addition to shock-wave propagation free surface flow instabilities must be controlled. Here upstream travelling surface waves could potentially disturb the surface unacceptably. The speed of gravity waves can be estimated as sqrt(g h)=sqrt(10m/s^2 .15m)~1.2m/s where h is the height of the fluid layer, which is an upper bound for potential surface waves. Thus, the speed of surface waves is below the anticipated flow velocity, so that the free surface flow is supercritical with respect to surface waves and a hydraulic jump forms when the supercritical flow enters the pool and becomes subcritical. At the exit of the channel a horizontal plate is installed where the flow becomes subcritical prior to entering the pool. This measure completely decouples the pool from the target.

Containment

The modular target is installed in a double-wall containment. The gap between the walls is filled with a cover-gas which is monitored for contamination. The Containment is build of material with small wall thickness. Low absorption cross section, low activation potential(anfällig), and sufficiently low gas production would be preferable. The containment is at ambient pressure and therefore is not subjected to high mechanical stresses. Using

suitable low activation materials the containment can be opened for maintenance with reasonable effort. Contamination of the containment by condensables like lead is suppressed by installing cold traps near any free surfaces and guiding vapour flow along the cold traps. The cold traps will stay operational in case of maintenance or replacement of modules, so that migration of activated materials is minimized when the containment is opened. The proton beam enters the containment trough a double safety window built from a suitable magnesium aluminium alloys and cooled by coolant like water. Evaporation cooling can realize high heat transfer. A break of the window is detected by adding tracers to the coolant which can be detected both in and outside the containment.

Preliminary thermohydraulic simulations

The mean flow and temperature distribution in the target module is computed using RANS (Reynolds averaged Navier Stokes). In the preliminary analysis the shock-absorbing flow obstacles in the channel are not considered. These obstacles will be optimized in a later step and allow to reduce the flow rate in those regions with small heat deposition. Figure 2.2 shows the simulated geometry and the employed boundary conditions. Clearly the pool geometry is strongly simplified.

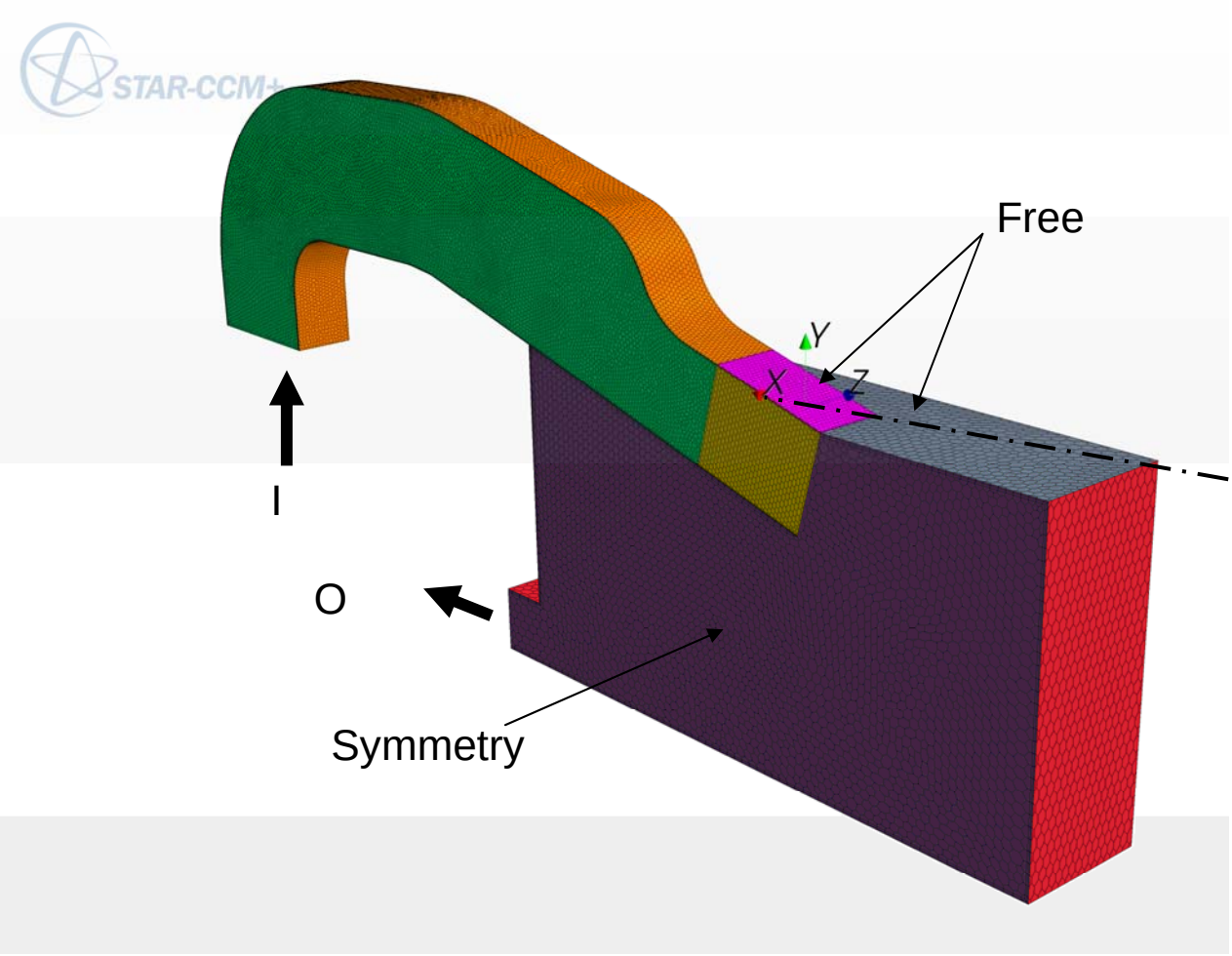

Fig.2.2: Computational domain, boundary conditions and mesh

The calculation assumes the following conditions:

Proton beam energy deposition: (M.Majerle, 2010)

Average jet velocity:	1-2 m/s (30-60 m3/h)
Inlet temperature:	200°C
Boundary conditions:	- adiabatic walls; - symmetry in Z-direction - no slip at walls - free surface
Fluid properties:	LBE, $(\nu,\sigma,\rho,\lambda) = f(T)$
Calculation model:	K- ε High Reynolds number TM; Volume of Fluid (VOF) Method; Transient

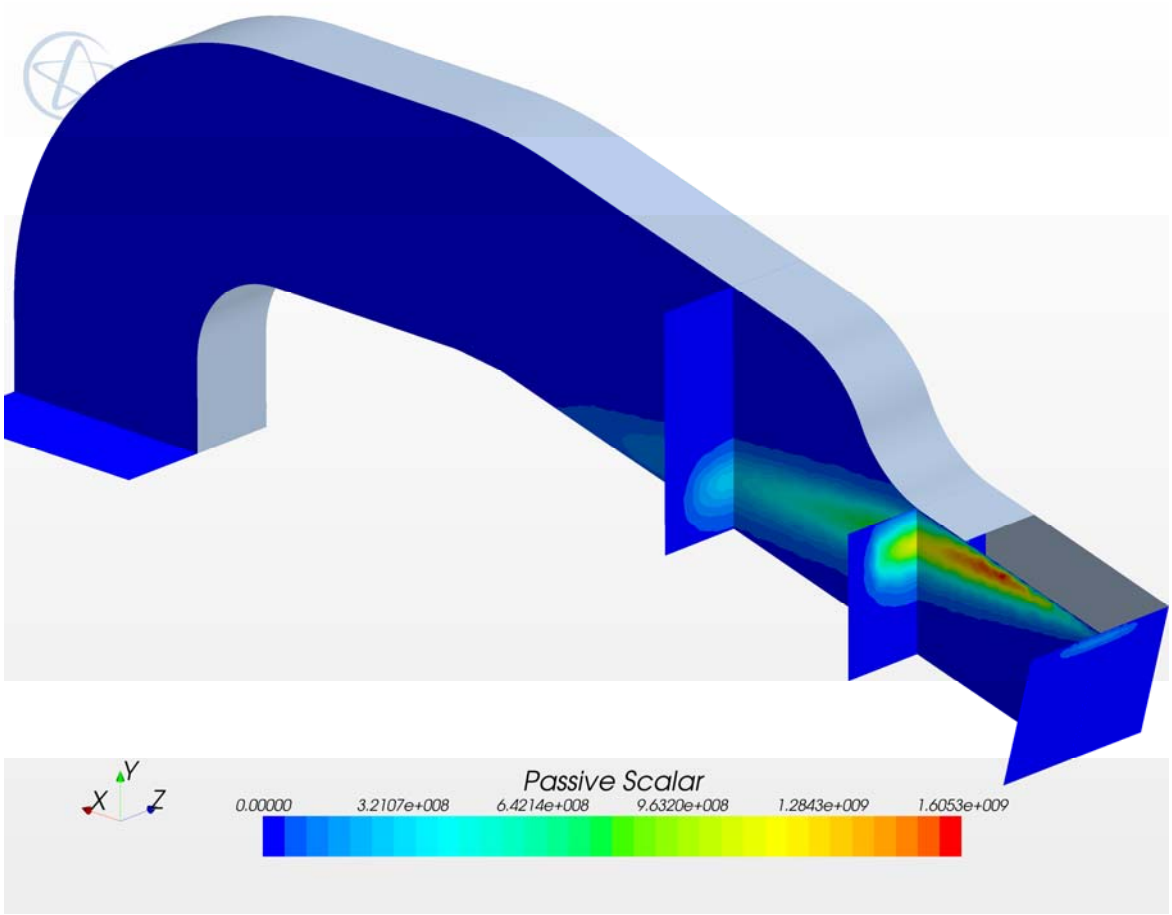

Fig. 2.3: Power density distribution as obtained by MCNPX-calculations

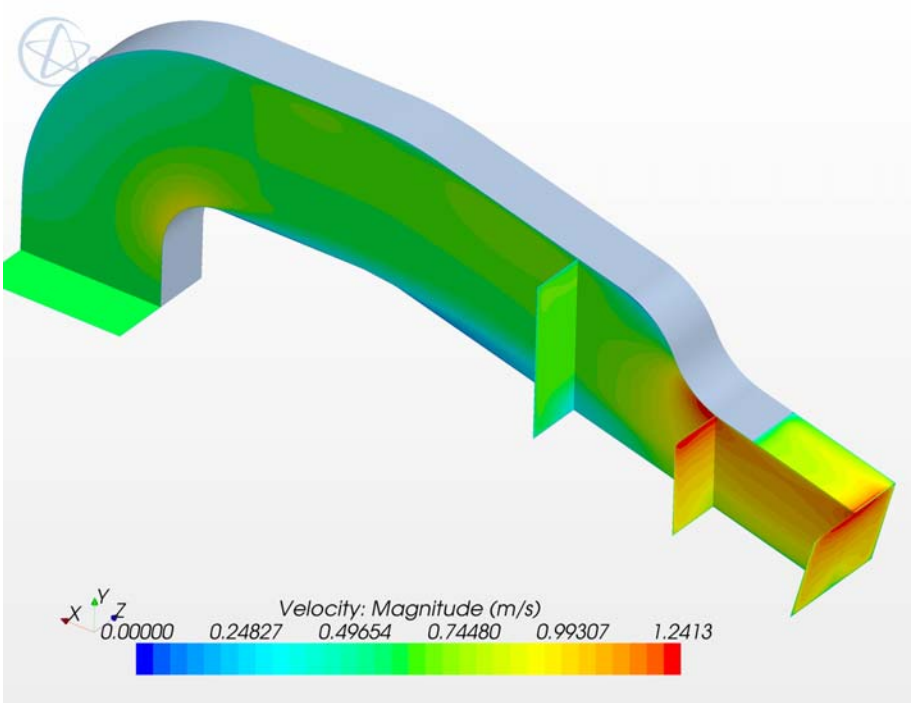

Fig. 2.4a: Velocity distribution (V=1m/s)

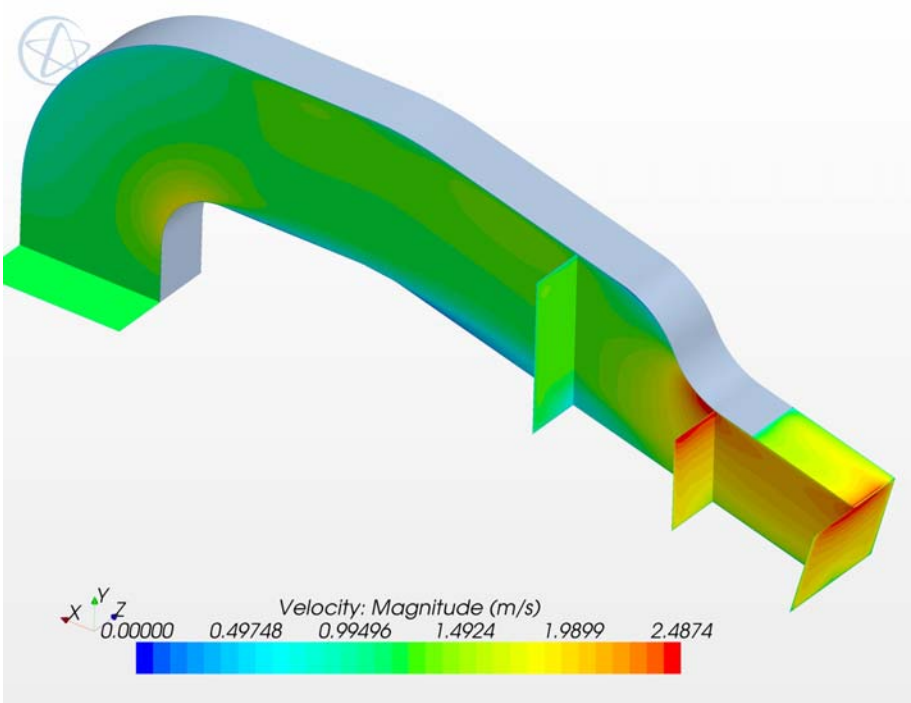

Fig. 2.4b: Velocity distribution (V=2m/s)

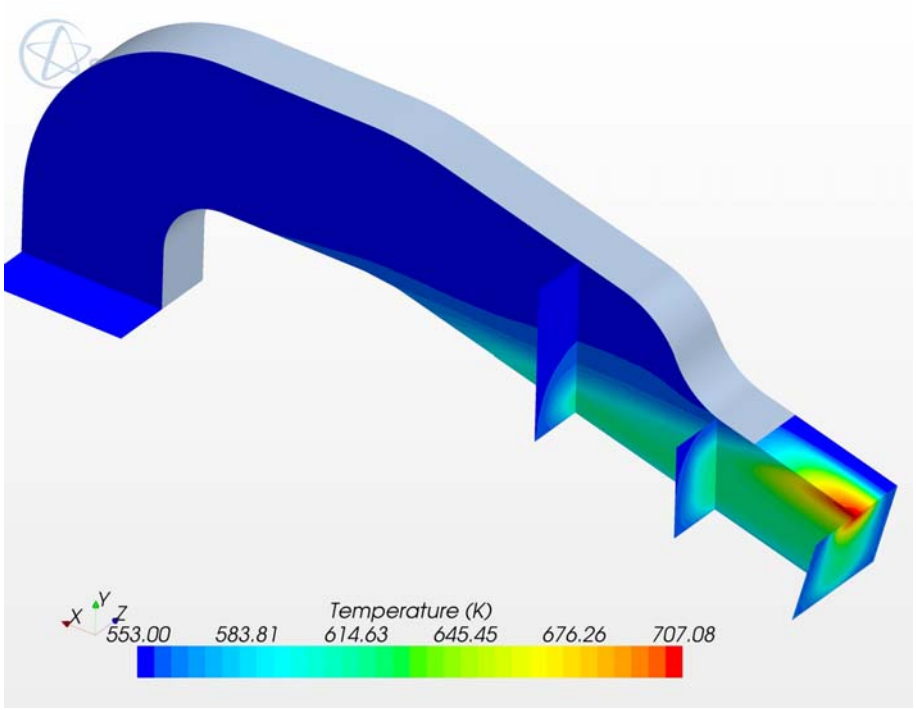

Fig. 2.5a: Temperature distribution (V=1m/s)

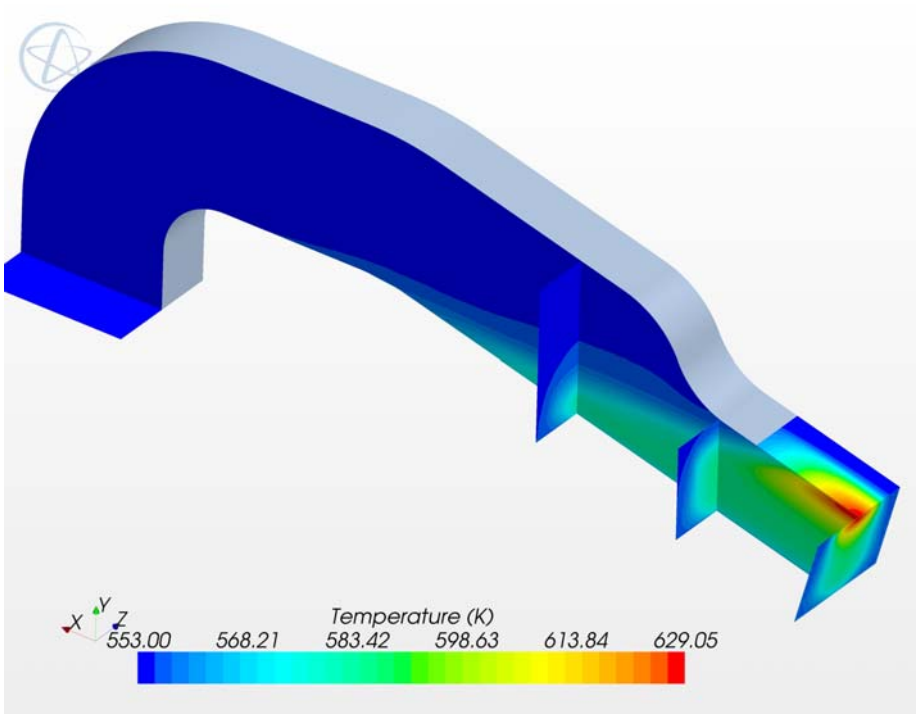

Fig. 2.5b: Temperature distribution (V=2m/s)

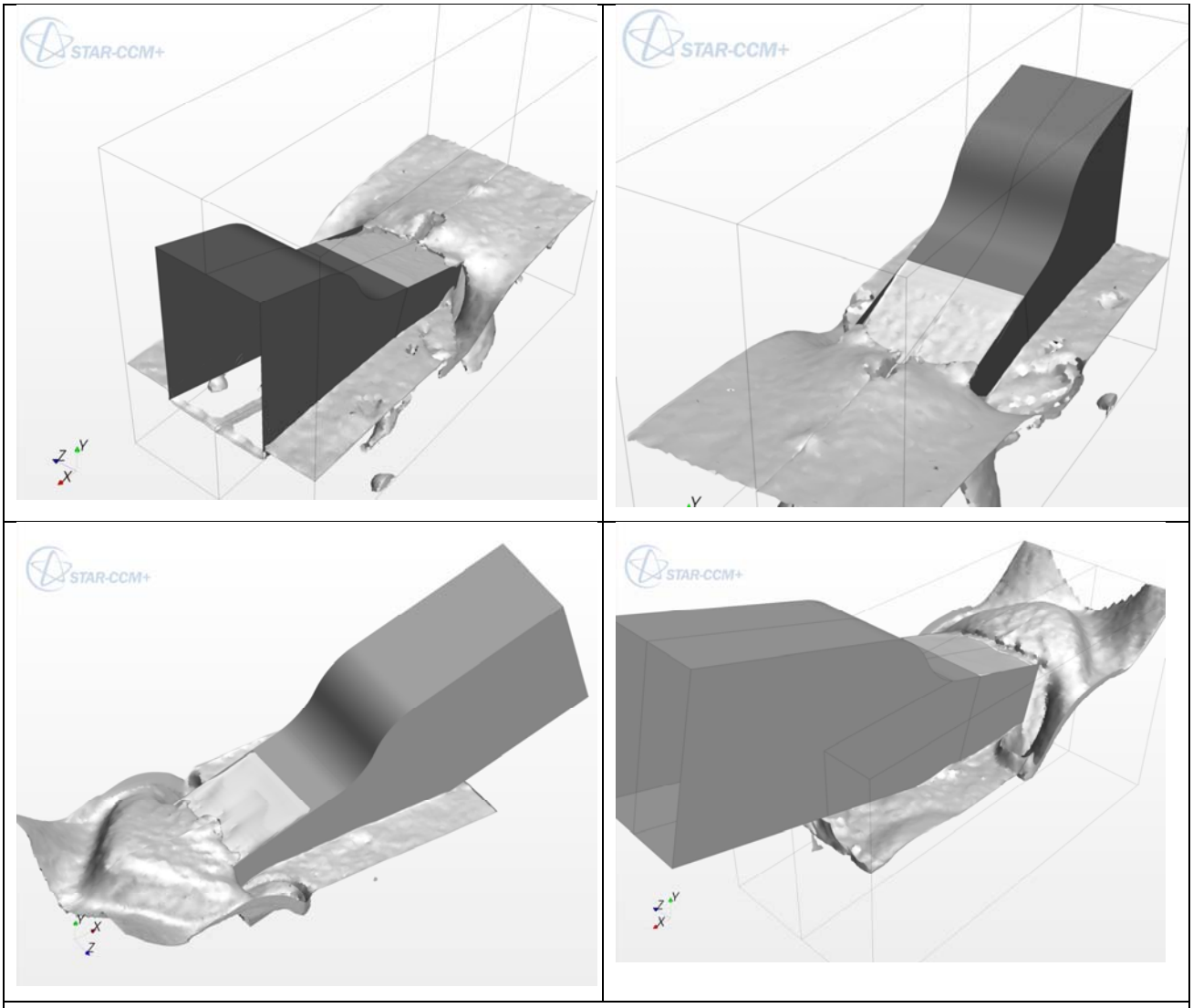

Fig. 2.6: Development of the free surface in the beam area

3 Neutronics

Neutronics calculations were performed with the MCNPX Monte Carlo code, version 2.7a, using the CEM nuclear cascade model. The calculations were performed on a Linux computer cluster running MCNX in the parallel mode under the MPI communication technique. Typically 10 million source particle histories were tracked in a calculation run providing in fractional standard deviations (FSD) in the range of a few percent or less. Results for the p- and n-fluxes, the heating, the dpa and gas production were generated on a fine regular mesh grid superimposed on the actual geometry using MCNPX's mesh tally capability.

A dedicated effort was spent on evaluating the cross-section data for the proton and neutron induced radiation damage (dpa) and gas production reactions up to 2.5 energy GeV

3.1 Generic analyses

Cylindrical PbBi target with 15 cm radius and variable length, pencil type proton beam impinging perpendicular on target front surface; proton beam energy varied from 500 MeV to 2.5 GeV.

Proton beam range

Increases linearly with proton beam energy (≈ 20 cm for 500 MeV, 80 cm for 1.3 GeV, and 180 cm for 2.5 GeV), see Fig. 3.1. Good agreement between MCNPX and SRIM calculations (Note this is for the proton slowing down by ionization processes, no nuclear interactions !).

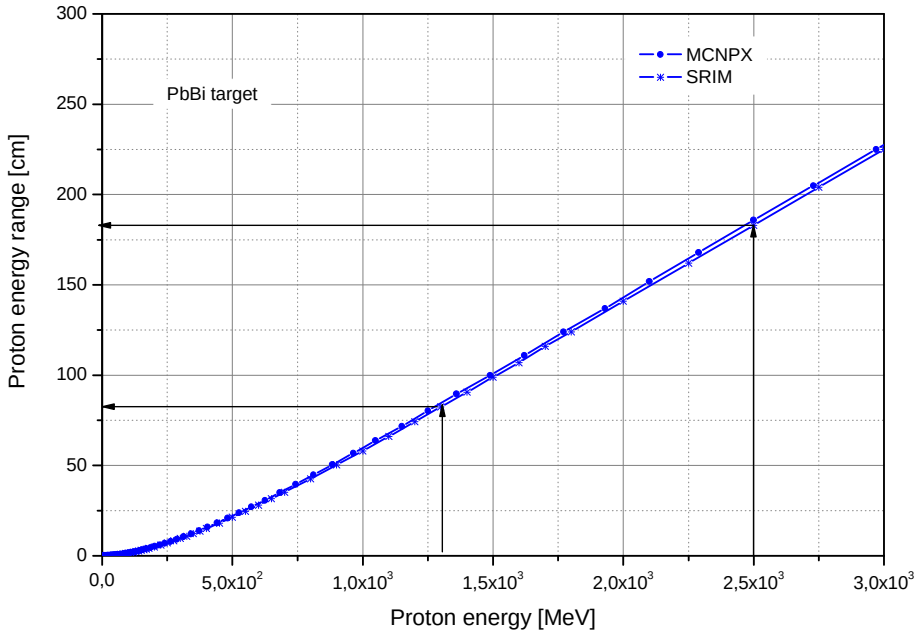

Fig. 3.1: Proton energy range in PbBi as function of proton energy

Such a large penetration depth is actually not required for the target since enough nuclear interactions take place already at smaller penetration depths (average mean free path for nuclear interactions of 500 – 2500 MeV protons inPbBi is around 18 cm)

The neutron yield actually saturates at a pentration depth of 80 to 100 cm, see Fig. 3.2 for the considered case of 2500 MeV protons. From this point of view, the PbBi target length can be therefore limited to 80 – 100 cm as mentioned above.

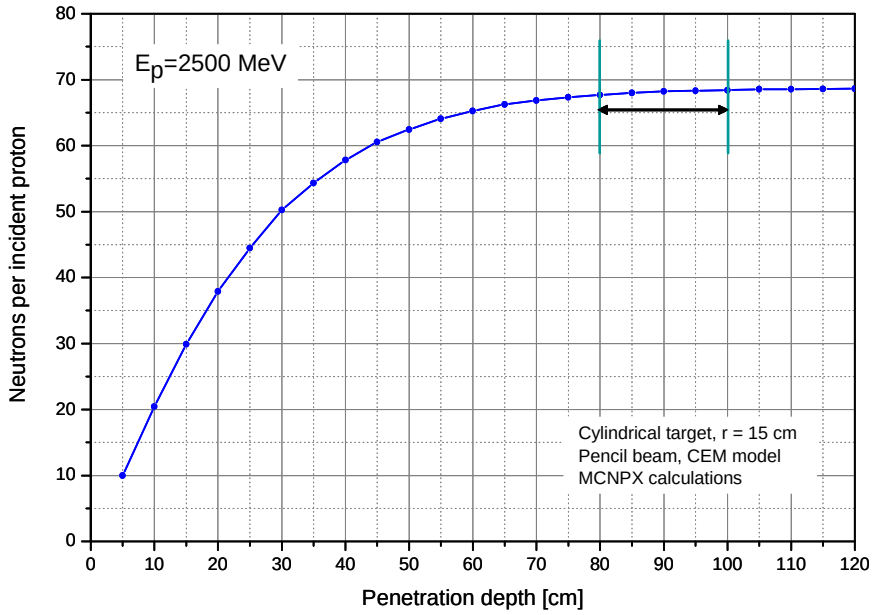

Fig. 3.2: Neutron yield for 2500 MeV proton in PbBi as function of the penetration depth

The impact of the incident proton beam energy on the neutron yield is shown in Fig. 3.3 for the PbBi cylindrical target with a length of 100cm. There is roughly a gain of a factor 2 in the neutron yield by increasing the proton beam energy from 1.3 to 2.5 GeV.

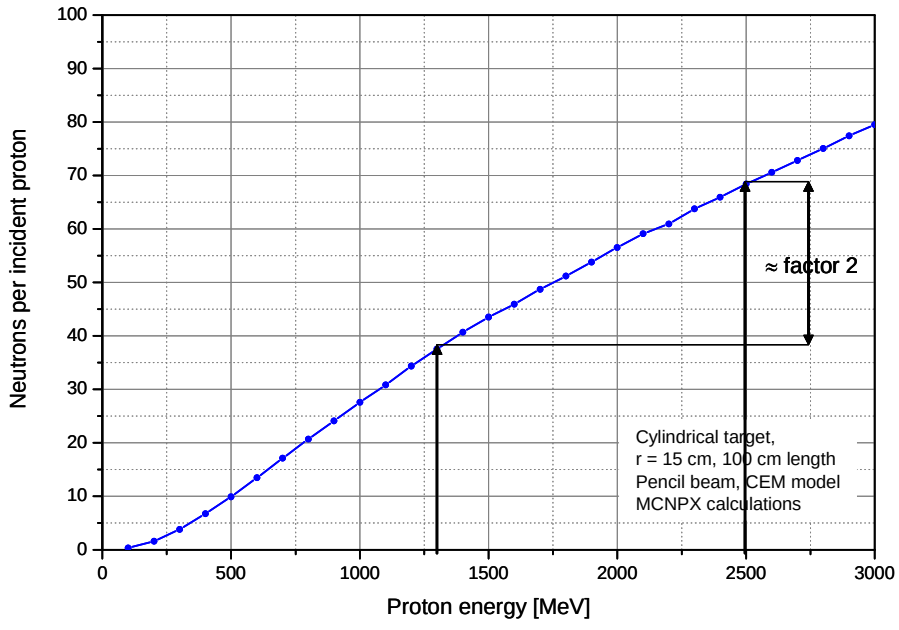

Fig. 3.3: Neutron yield for protons in PbBi as function of incident proton energy

Fig. 3.4 compares the proton flux profiles along the target depth for 0.5, 1.0, 1.5 and 2.´5 GeV proton beam energies. There is clearly visible a steep drop-off by two to three order of magnitude once the proton (ion) range has been reached. The proton flux beyond the indicated

proton (ion) range is due to the protons generated in the previous nuclear interactions of the hadrons and the PbBi.

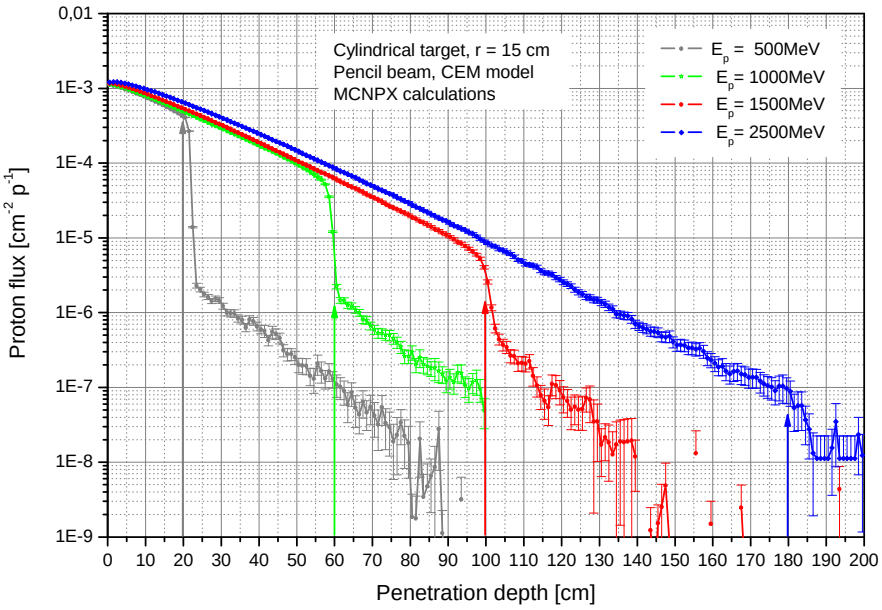

Fig. 3.4: Proton flux density profiles in PbBi as function of the penetration depth.

Fig. 3.5 shows neutron flux profiles along the central axis up to 100 cm penetration depth for 1.5 and 2.5 GeV proton beam energies. The gain in the neutron flux (2.5 vs. 1.5 GeV proton beam) is around 30 % in the front region, where there is the neutron flux maximum, and up to a factor 2 to 3 at penetration depths of 80 to 100 cm. Thus there is an apparent benefit in terms of an increased neutron flux density level by increasing the proton beam energy from 1.5 to 2.5 Geb. Note, however, that the neutron flux density level at the far end of the target is by about three orders of magnitude lower than in the front area.

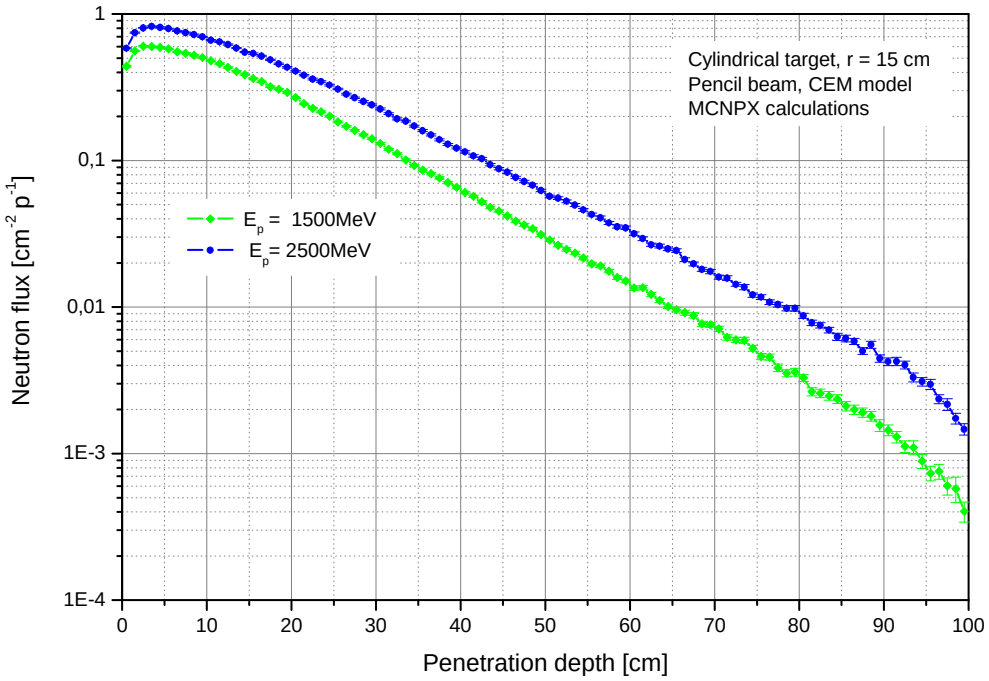

Fig. 3.5: Neutron flux density profiles in PbBi along the central axis

3.2 Evaluation of neutron and proton induced dpa and gas production cross-section data for Fe, Cr, Ni up to 2.5 GeV

Brief explanation of method, in particular for DPA cross-section evaluation; plots for dpa and He production.

Proton and neutron induced displacement damage cross-section data were evaluated up to 2.5 GeV for the steel constituents Fe, Cr and Ni. Two different approaches have been applied, the standard NRT model, and an advanced method based on molecular dynamics (MD) combined with binary approximation model (BCA) simulations.

Data can be made available, ENDF type data files as well as process input data for MCNP/MCNPX

In the following, we show some plots for the dpa cross-sections (gas production cross-sections to be added)

Neutron induced	**Proton induced**

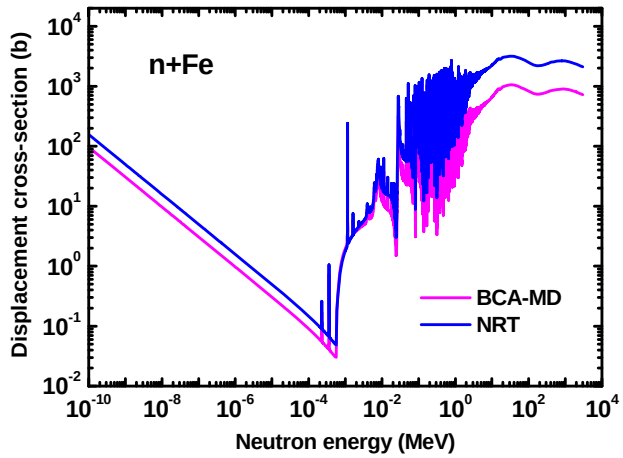

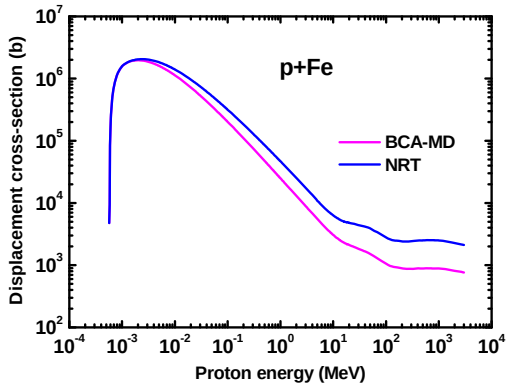

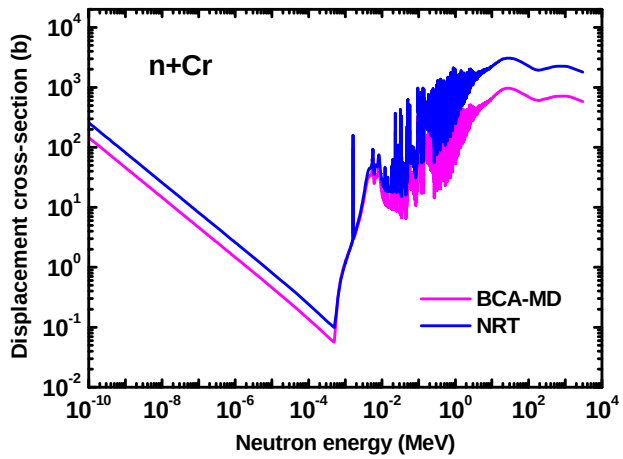

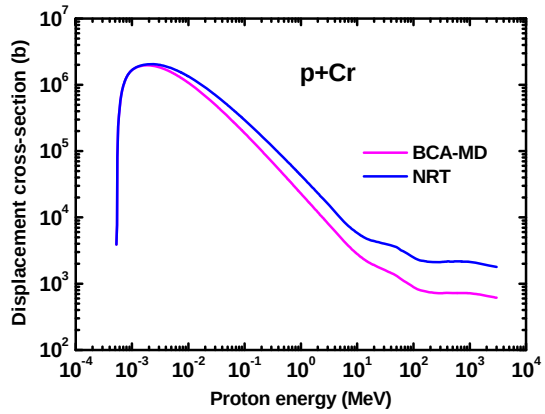

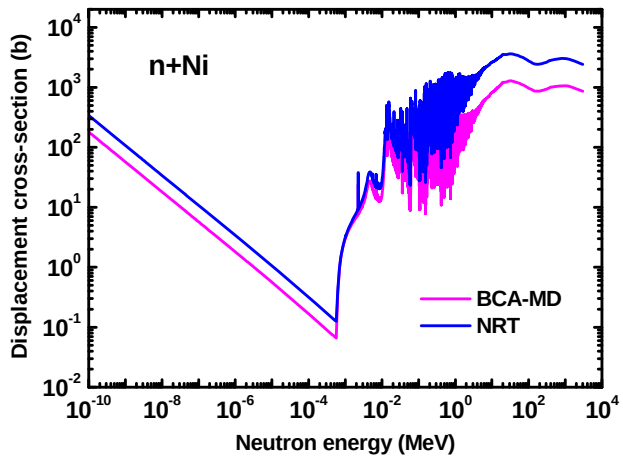

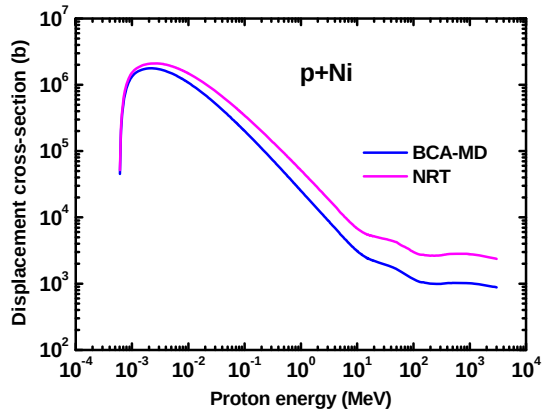

Evaluated displacement damage cross-section data for neutron and protons up to 2.5 GeV

3.3 Dedicated analyses for the WITA target design

A simplified model of the simplified WITA target design was devised for the neutronic calculations with the MCNPX code, see Fig. 3.6. The model consists of a steel frame filled with PbBi and a free surface where the proton beam impinges under an angle of 15°. The proton beam has been modelled according to the specification given by D. Ene, C. Kharoua, E. Noah and F. Plewinskii, in "Proton beam parameter list for ESS target design, ESS document, Ref: 10817v.3, 5 July 2010", i. e. assuming a Gaussian profile with a beam width of 200 mm, beam height of 60 mm, horizontal sigma ($w_b = 4\ \sigma_x$) of 50 mm and vertical sigma ($h_b = 4\ \sigma_y$) of 15 mm, proton beam energy of 2.5 GeV and an average beam current of 2mA.

Two dedicated scoring regions in the side and bottom walls were defined for assessing damage and gas production in the steel structure as shown in Fig. 3.6.

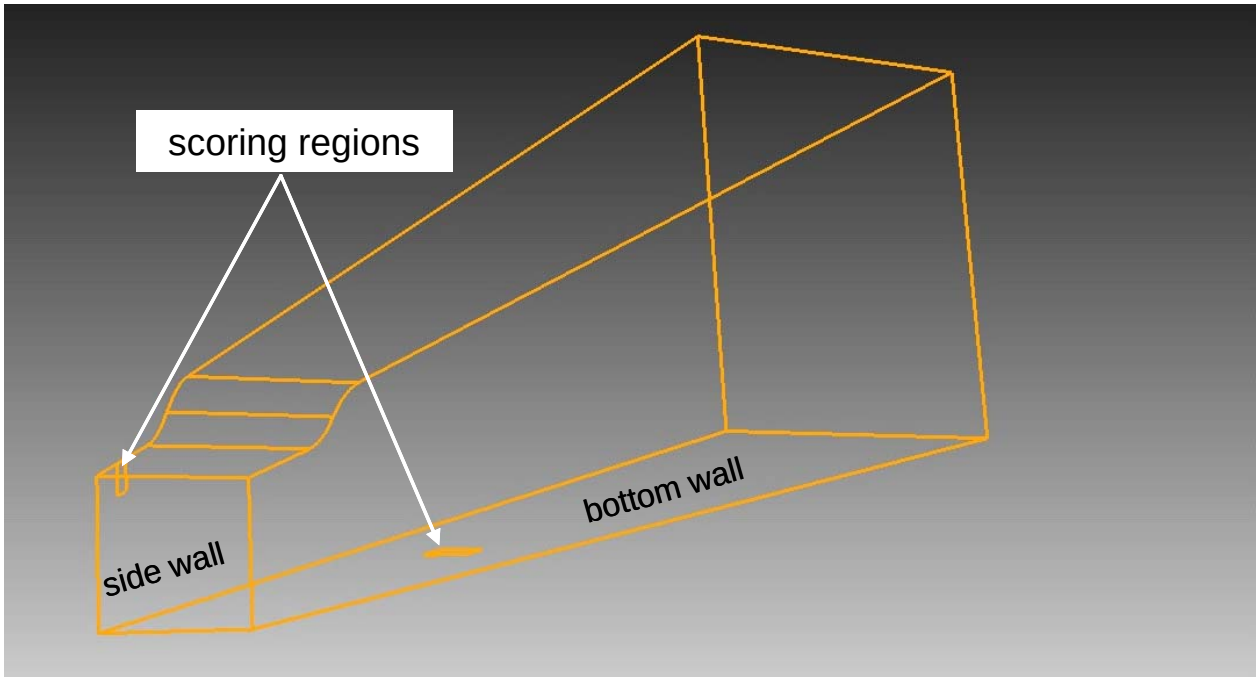

Fig. 3.6: Sketch of WITA target model used for neutronics calculations with scoring regions in side and bottom walls indicated

Nuclear heating, neutron and proton flux distributions were calculated on a fine regular mesh grid in the PbBi target. Fig. 3.7 shows 2d contour maps in a vertical midplane in beam upward direction. The maximum power density in the PbBi amounts to about 1000 Wcm-3. The maximum values of the proton and neutron flux densities are in the range of 10^{15} and 10^{16} $cm^{-2}s1$, respectively.

As noted above, damage and gas production rates in steel were calculated in the side and bottom walls again on a fine regular mesh grid centred around the two dedicated scoring regions. Displacement damage and gas production rates (H, He) were based on the corresponding proton and neutron induced cross-section data evaluated in up to 2.5 GeV for the steel constituents Fe, Cr and Ni. In the case of displacement damage, the standard NRT model has been used for evaluating the dpa cross-section data. In addition, an advanced method has been utilized to provide displacement cross-section data on the basis of molecular dynamics (MD) combined with binary approximation model (BCA) simulations. This approach results in lower dpa rates (about a factor 3 in the case of ESS)

which are, however, more reliable than the NRT based dpa rates. Dpa and gas production rates were calculated for one full power year (fpy) operation of ESS (NB. In general 5000 hours full power operation are assumed; this is a bit more than half a year). The maximum damage rate (side steel wall) is around 14 dpa (NRT), maximum He production is at 200 appm and maximum H prodction at 1000 appm. Figs. 3.24 -3.27 show contour maps of the dpa (NRT) broken down in contributions induced by protons and neutrons.

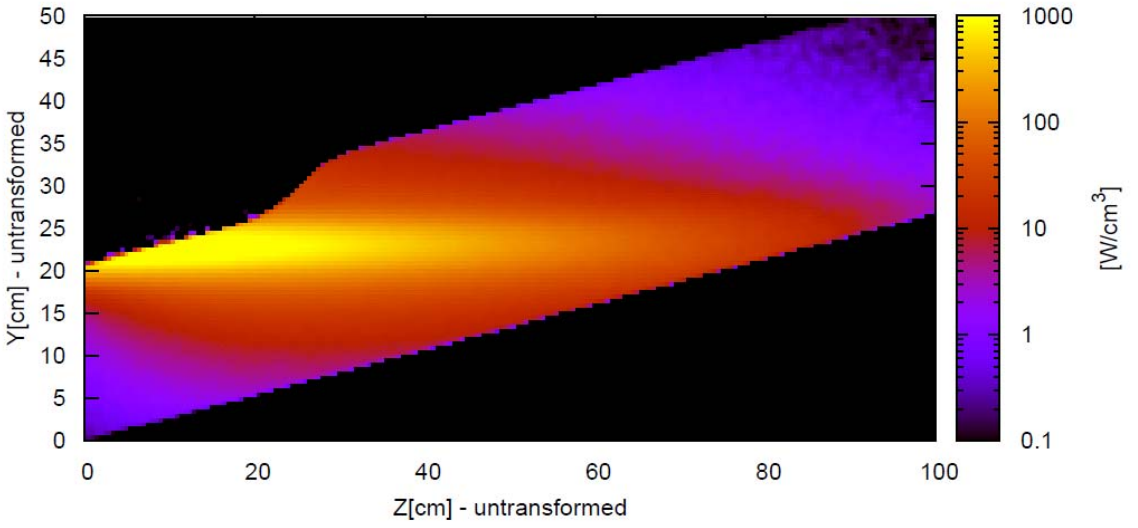

Fig. 3.7: Heating power density distribution in PbBi [Wcm^{-3}]

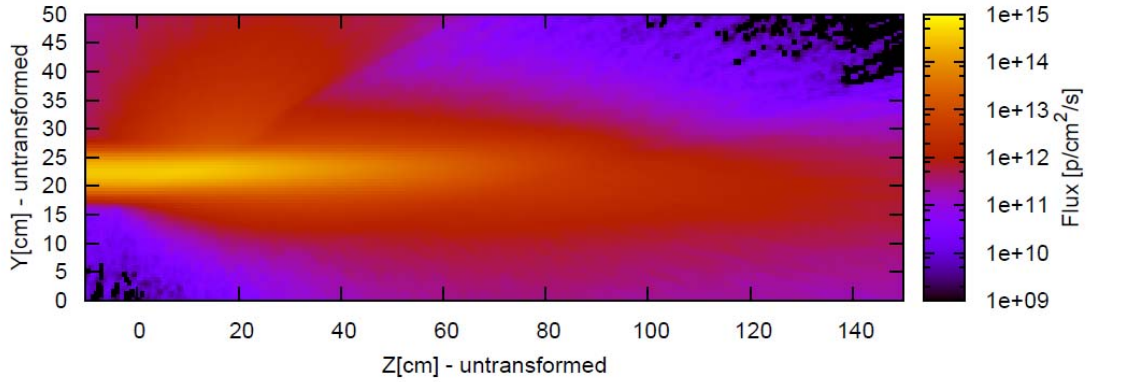

Fig. 3.8: Proton flux density distribution in PbBi [$cm^{-2}s^{-1}$]

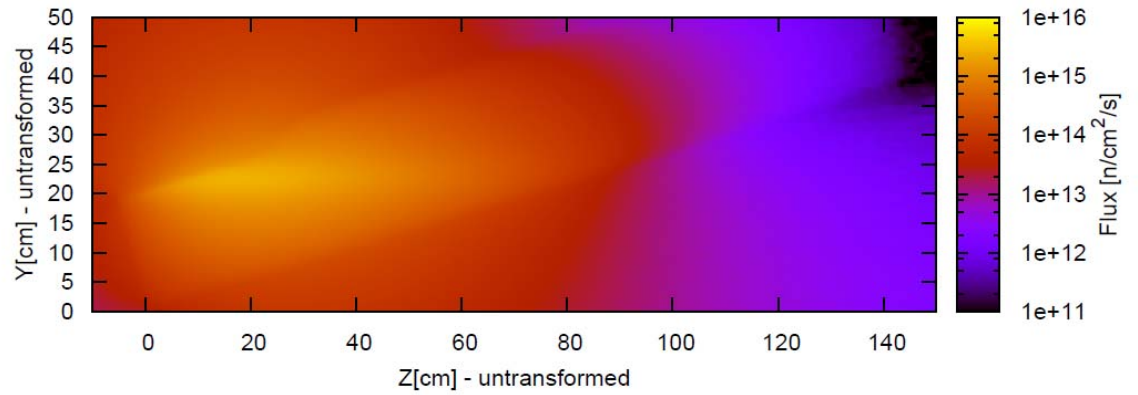

Fig. 3.9: Neutron flux density distribution in PbBi [$cm^{-2}s^{-1}$]

Displacement damage and fast neutron flux distribution in side steel wall

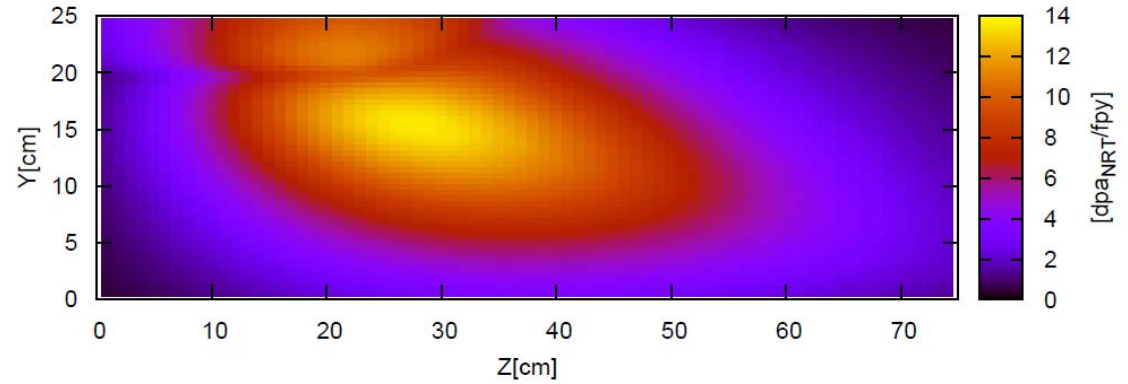

Fig. 3.10: Distribution of dpa_{NRT} accumulation (1 full power year)

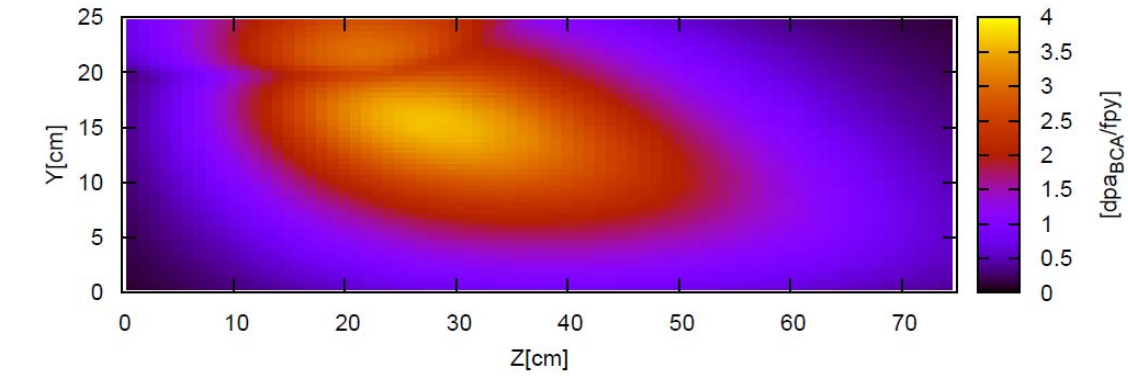

Fig. 3.11: Distribution of dpa_{BCA} accumulation (1 full power year)

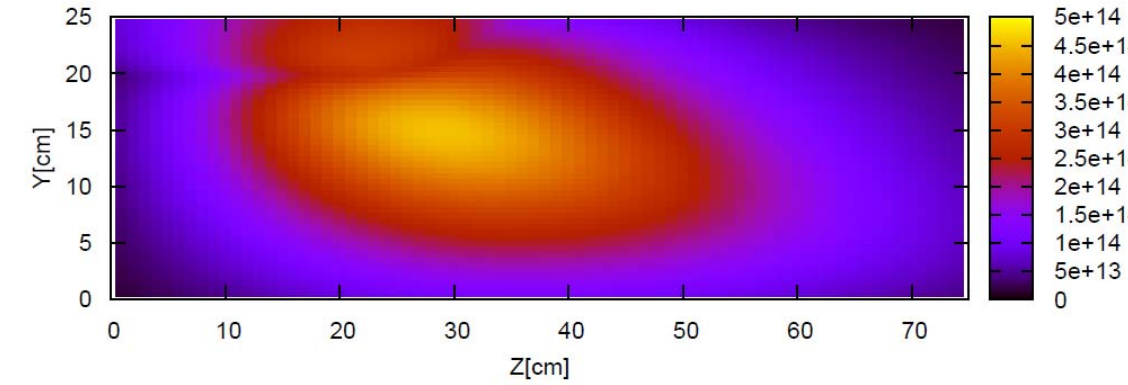

Fig. 3.12: Distribution of fast (E>0.1 MeV) neutron flux density [$cm^{-2}s^{-1}$]

Displacement damage and fast neutron flux distribution in bottom steel wall

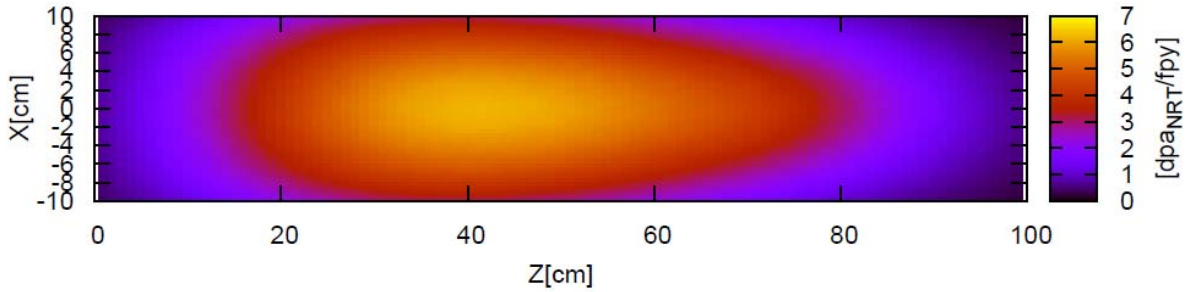

Fig. 3.13: Distribution of dpa_{NRT} accumulation (1 full power year)

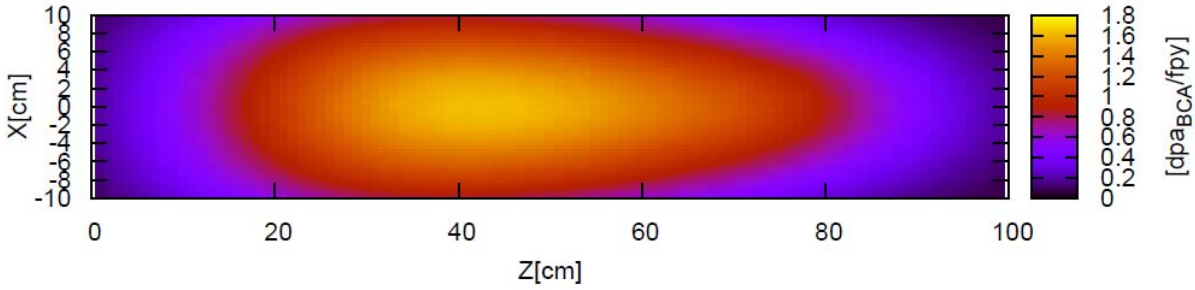

Fig. 3.14: Distribution of dpa_{BCA} accumulation (1 full power year)

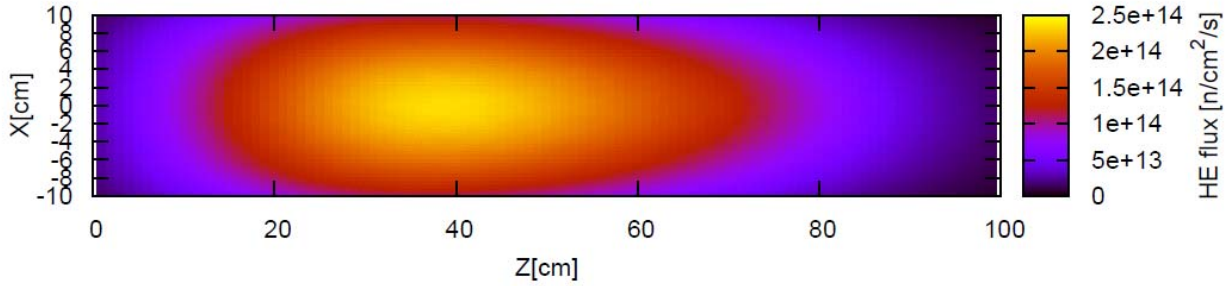

Fig. 3.15: Distribution of fast (E>0.1 MeV) neutron flux density [$cm^{-2}s^{-1}$]

Helium and hydrogen production in side steel wall

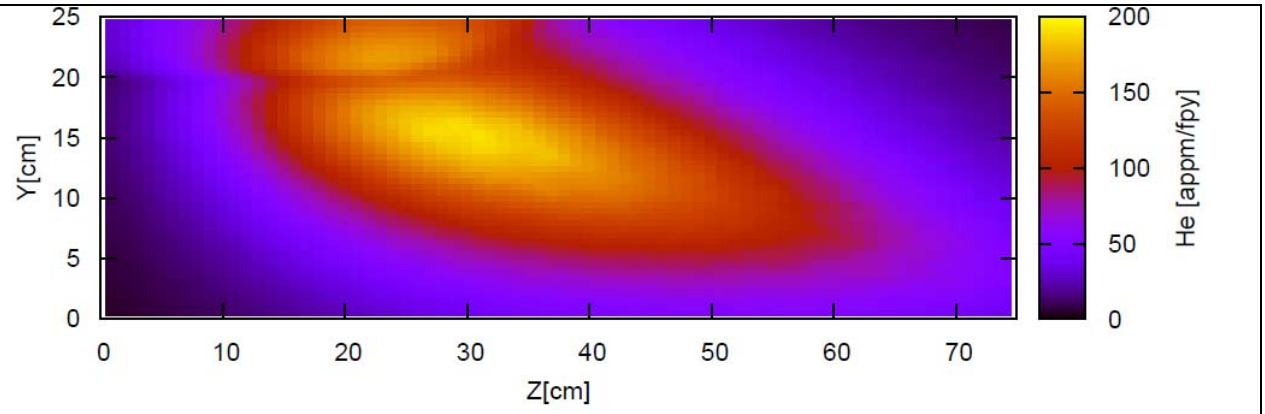

Fig. 3.16: Distribution of He production (appm per full power year)

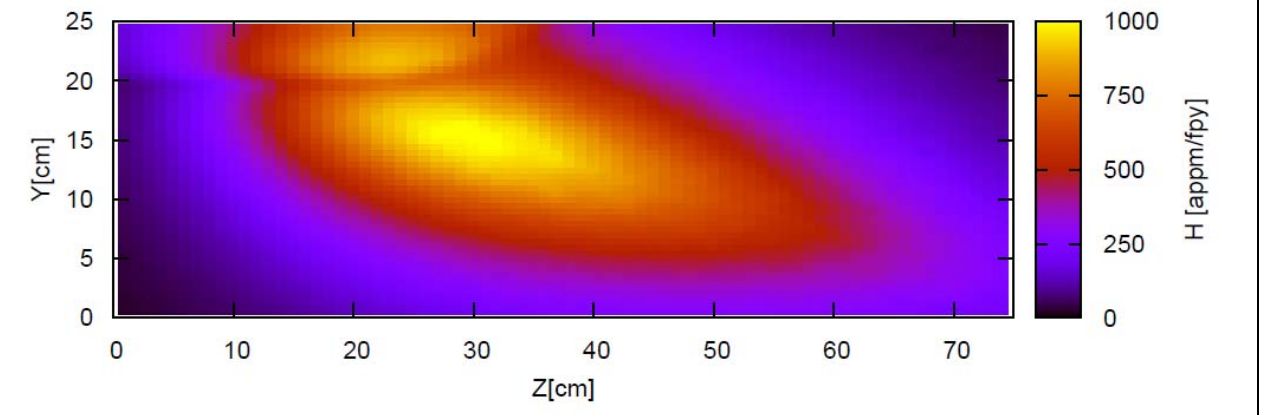

Fig. 3.17: Distribution of H production (appm per full power year)

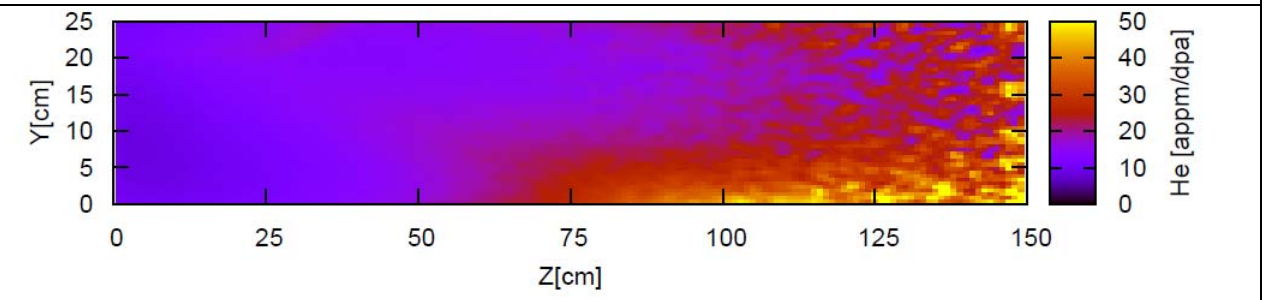

Fig. 3.18:Ratio He production/dpa accumulation (appm He/dpa)

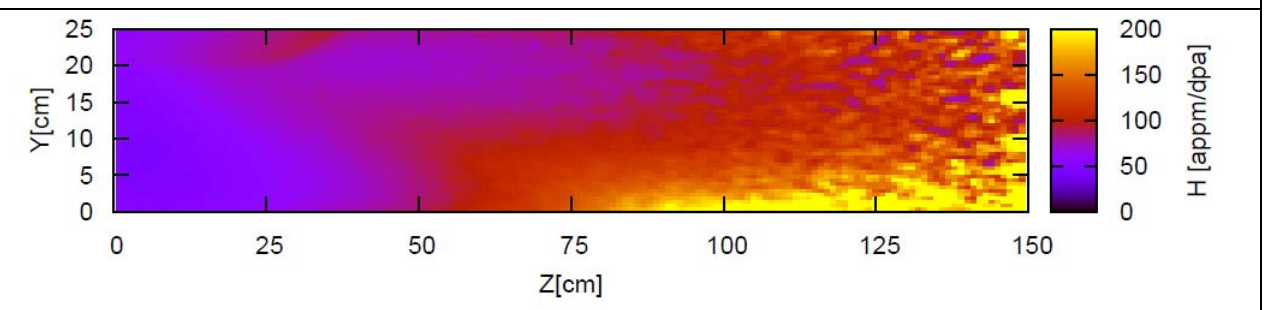

Fig. 3.19: Ratio H production/dpa accumulation (appm He/dpa)

Helium and hydrogen production in bottom steel wall

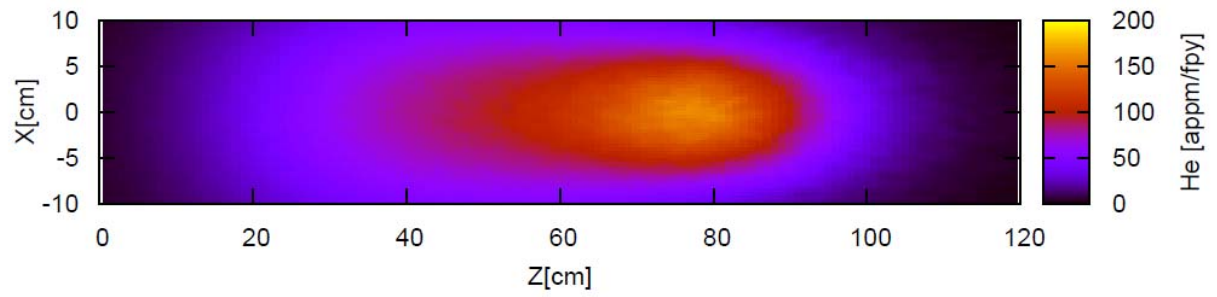

Fig. 3.20: Distribution of He production (appm per full power year)

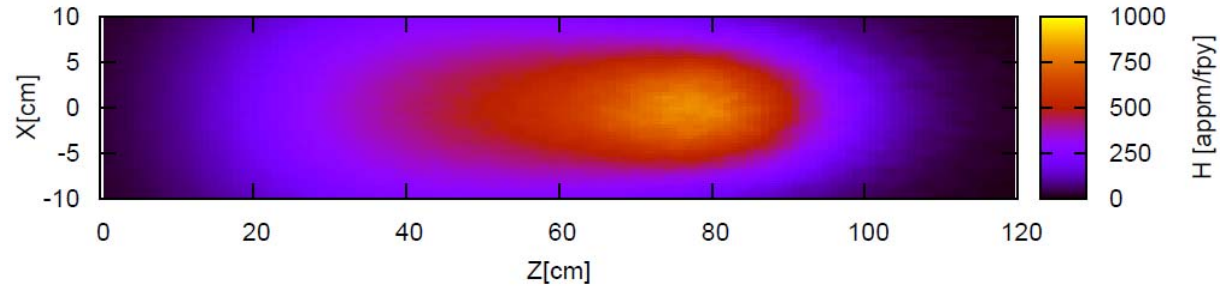

Fig. 3.21: Distribution of H production (appm per full power year)

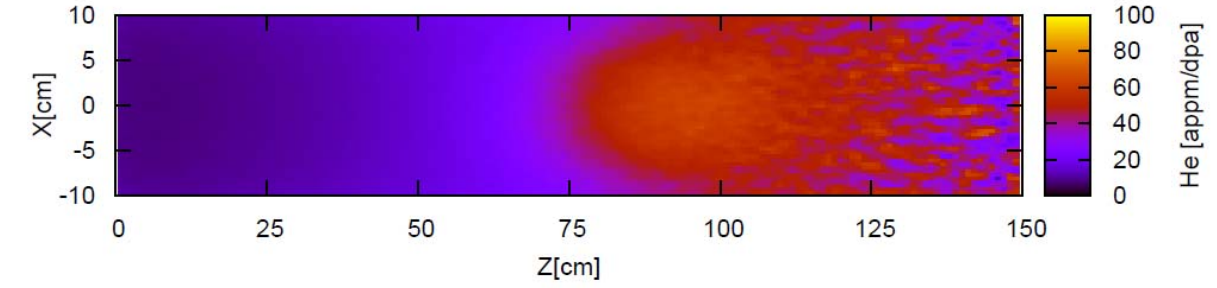

Fig. 3.22:Ratio He production/dpa accumulation (appm He/dpa)

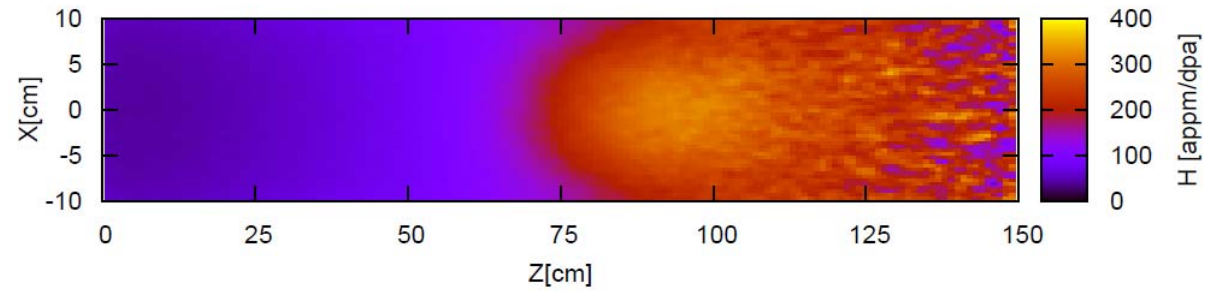

Fig. 3.23: Ratio H production/dpa accumulation (appm He/dpa)

Proton and neutron induced damage accumulation in steel walls

Side wall

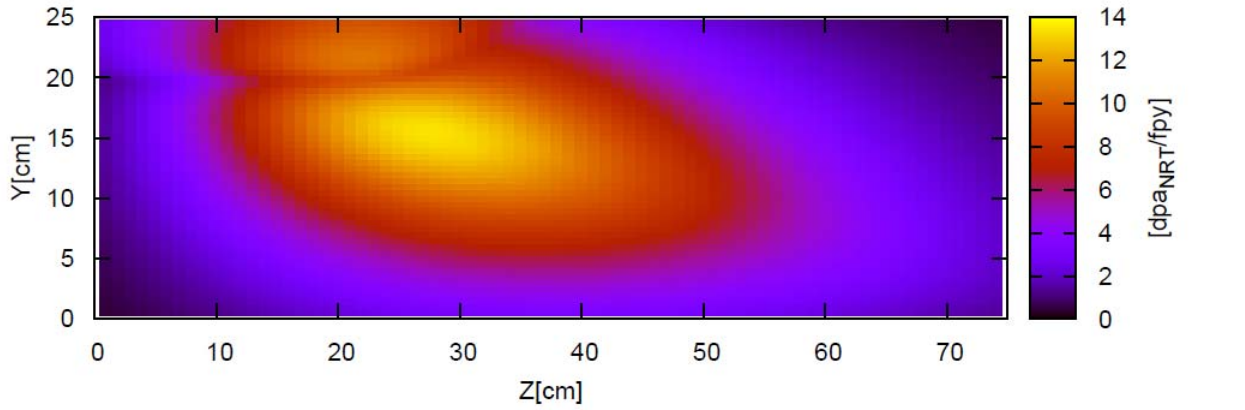

Fig. 3.24: Neutron induced dpa$_{NRT}$ accumulation (1 full power year)

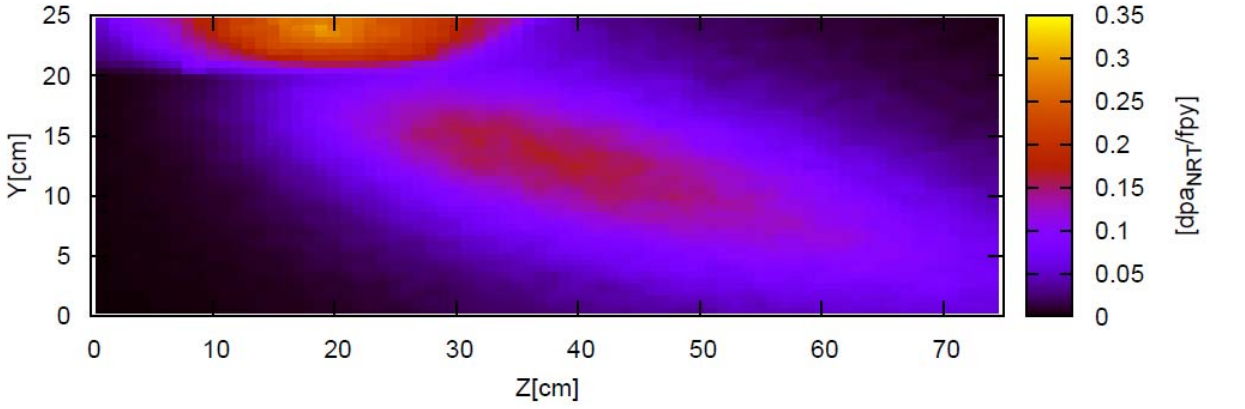

Fig. 3.25: Proton induced dpa$_{NRT}$ accumulation (1 full power year)

Bottom wall

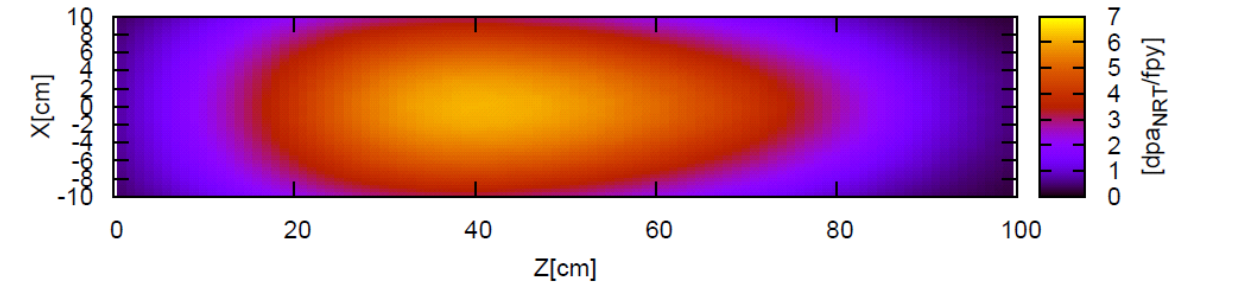

Fig. 3.26: Neutron induced dpa$_{NRT}$ accumulation (1 full power year)

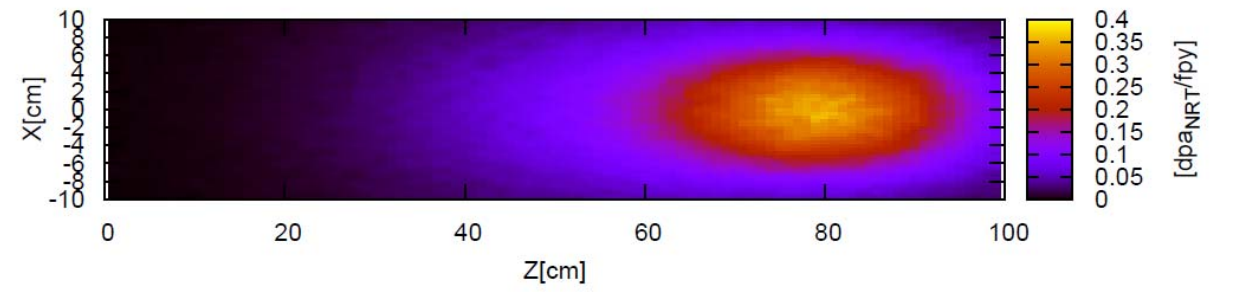

Fig. 3.27: Proton induced dpa$_{NRT}$ accumulation (1 full power year)

4 Material issues

4.1 Operation conditions

LBE working temperature is assumed to be 280°C. Beam heating will result in <~70°C increase of the LBE temperature. Therefore the range of operation temperatures of structural materials of the flow guide and LBE tray is 280-350°C.

Neutronics calculations give a preliminary assessment of irradiation conditions (Fig. 4.1-4.3). The maximum displacement damage rate of 14 dpa/year is reached on the side faces of the flow guide, while two times lower dose (7 dpa/fpy) is expected at the bottom face. Gas production rates at flow guide faces are rather high: 1000 appm H/fpy and 190 appm He/fpy for the side face and 900 appm H/fpy and 180 appm He/fpy for the bottom face.

These values should be compared with that for ADS beam window and for ESS target.

The data above correspond to the gas to damage ratio of 70 appm H/dpa and 14 appm He/dpa for the side face and 128 appm H/dpa and 27 appm He/dpa for the bottom face.

Upper face is being examined now.

	ADS	**ESS 2003**		**ESS Sweden 2010**		
E_p, MeV	600	1.3		2.5		
I, mA	2.46	3.75		2		
P, MW	1.5	5		5		
Position	beam window	target	reflector	Flow guide side wall	Flow guide bottom wall	Flow obstacles
Damage rate, dpa/fpy	32	33	10	14	7	
Hydrogen production, appm H/fpy	9×10^3	5×10^4	360	1000	900	
Helium production, appm He/fpy	1.4×10^3	1000	60	190	180	
appm H/dpa	280	300	36	70	128	
appm He/dpa	44	30	6	14	27	

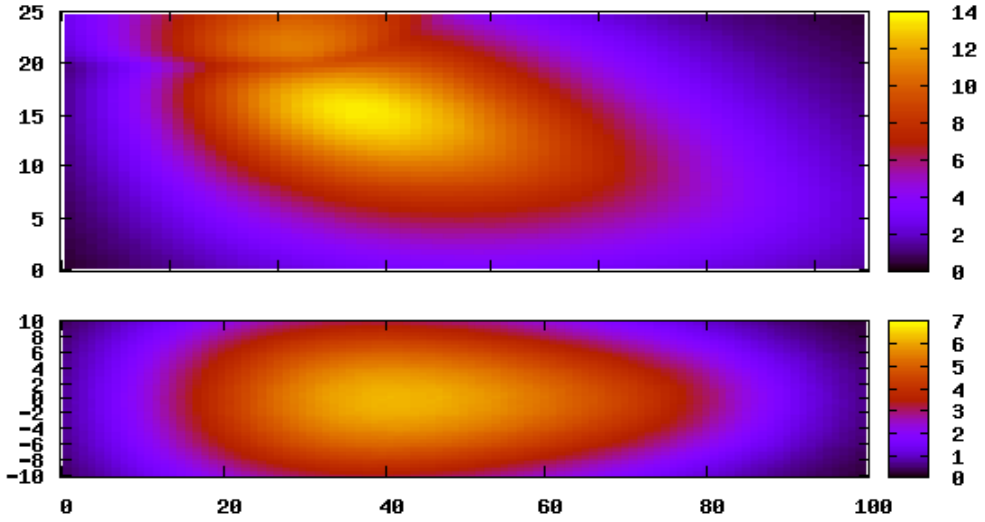

Fig. 4.1: Displacement damage rate according to NRT (in dpa/fpy) calculated in 316SS on the side (upper) and bottom (lower) walls of the flow guide

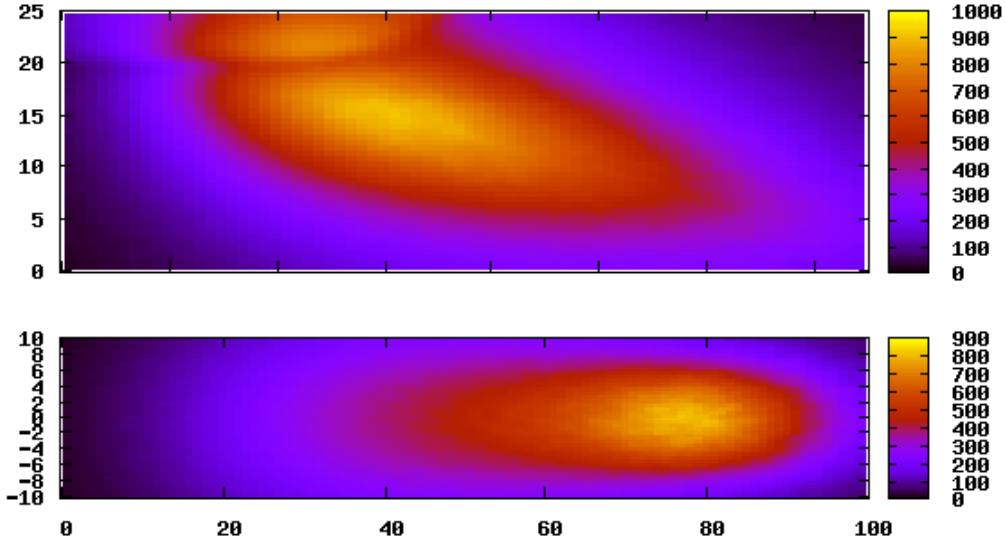

Fig. 4.2: Hydrogen production (in appm H/fpy) calculated in iron on the side (upper) and bottom (lower) walls of the flow guide

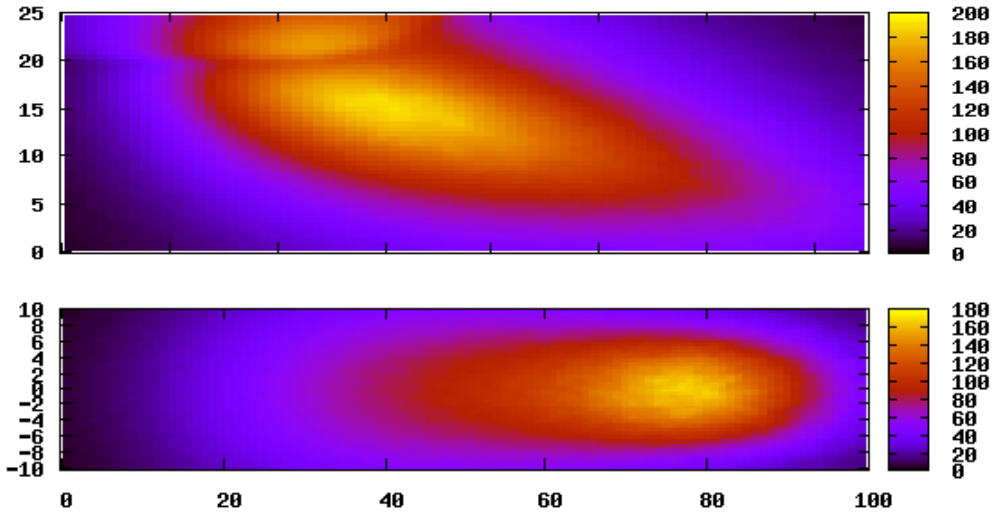

Fig. 4.3: Helium production (in appm He/fpy) calculated in iron on the side (upper) and bottom (lower) walls of the flow guide

Two general classes of structural materials are widely used for nuclear applications: austenitic steels and ferritic-martensitic steels. Under irradiation the first one has relatively short-time delay for swelling in the temperature range 300-650°C, while the second one is susceptible to embrittlement. Austenitic steels possess shorter delay or incubation time before stationary swelling (0.1-10 dpa, for some commercial steels exceeds 100 dpa) than bcc materials. After reaching stationary regime both classes of steel swell with the same rate of ~1%/dpa which is nearly independent of initial impurities, initial dislocation density, system temperature, and irradiation dose-rate. On the contrary, the incubation period appears to depend on these parameters. In particular the delay of swelling is shorter for lower irradiation dose-rate. Being started swelling is rapidly degrading properties of material. Thus the incubation time defines mainly the useful lifetime of the reactor components.

The overall material behaviour under irradiation generally depends on combination of the major three factors: irradiation temperature, dose-rate and accumulated dose, which should also include accumulated amounts of gases produced by transmutation.

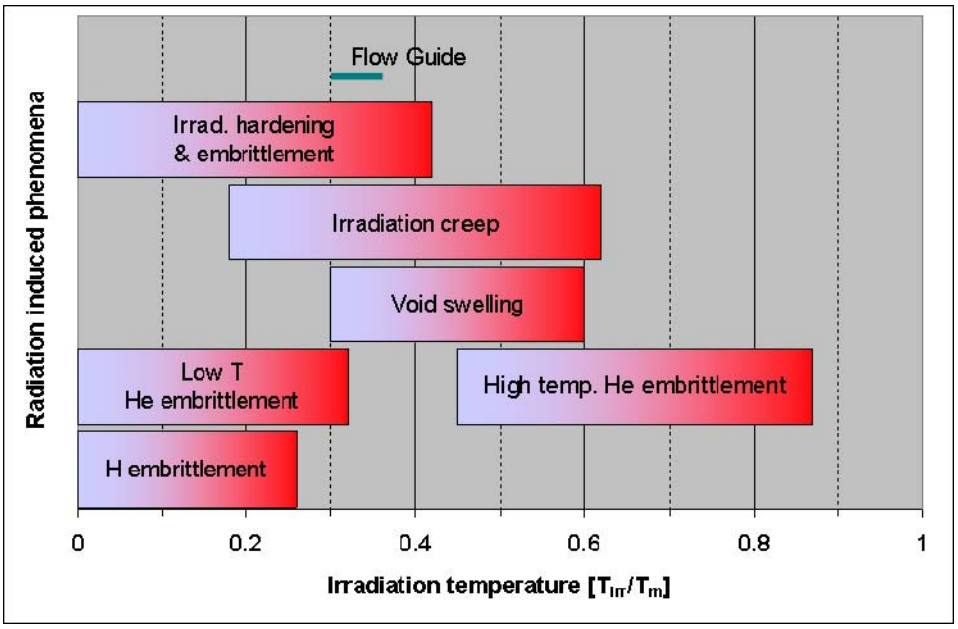

Fig. 4.4 Radiation induced phenomena and anticipated operation temperature windows of ESS flow guide.

Operation temperature range

The lower allowable temperature for the structural materials considered is determined by radiation induced hardening (fcc and bcc) and embrittlement (fracture toughness decrease for bcc materials), while the upper one is defined by one of the following reasons (Fig. 4.4.4) [Zink00]:

- Thermal creep (grain boundary sliding or matrix diffusion),
- High temperature helium embrittlement of grain boundaries
- Void swelling,
- Coolant compatibility / corrosion issues.
- Cavitation erosion
- Embrittlement due to spallation products

It should be noted that at temperatures below 500°C there is no remarkable corrosion of structural materials in LBE.

316LN Stainless steel

Main problem of this steel is complete loss of uniform elongation (strain to necking) after irradiation at 330°C already at 7-10 dpa (see Fig. 4.54.5). For this reason Type 316LN steel was not selected as structural material for the IFMIF target back plate which operates at 270-360°C, under irradiation with displacement dose rate of 60 dpa/fpy and helium accumulation rate of 600 appm He/fpy. Reduced activation ferritic-martensitic steel was selected for the IFMIF back plate and is proposed for the ESS flow guide. The temperature range of both components is practically the same, while displacement damage rate is for IFMIF higher.

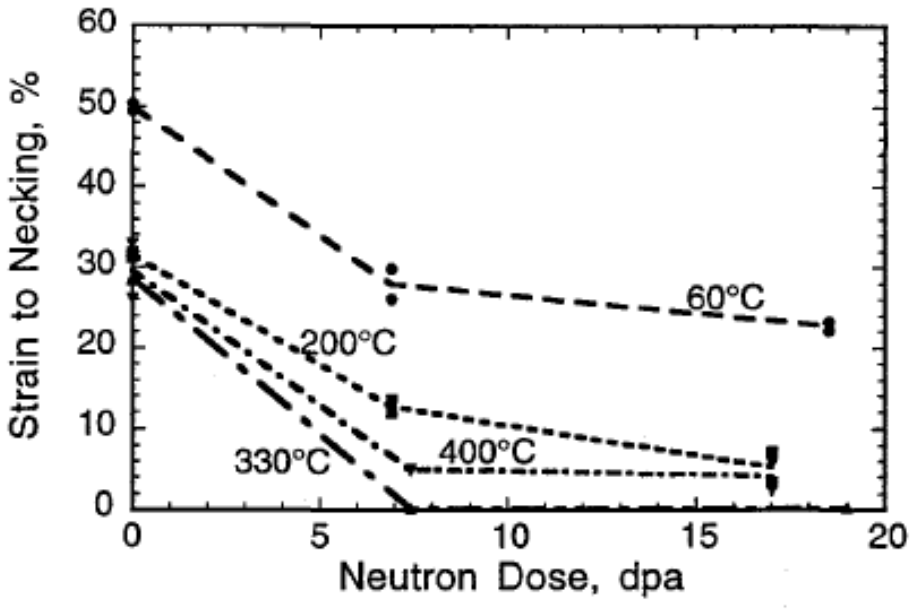

Fig. 4.5: Strain to necking as a function of neutron dose [Robe97]

EUROFER97

Radiation induced embrittlement is considered to be main problem of EUROFER97. Fig. 4.6 shows ductile to brittle transition temperature (DBTT) shift with irradiation dose for EUROFER97 irradiated in BOR-60 at 300-330°C. At maximum presently available dose of 70 dpa the irradiation induced shift is below 250°C. This means that even at 70 dpa the safety margin for impact fracture is more than 130°C.

Fig. 4.7 shows yield strength behaviour of 316SS irradiated in the temperature range of 0-200°C under spallation conditions, while the yield strength increase for various reduced activation ferritic-martensitic steels (including EUROFER97) neutron irradiated and tested at 300-325°C is shown in Fig. 4.8. By comparing both graphs one can find that radiation induced hardening is similar for both 316LN and EUROFER97 being 500-600 MPa after irradiation up to 40 dpa.

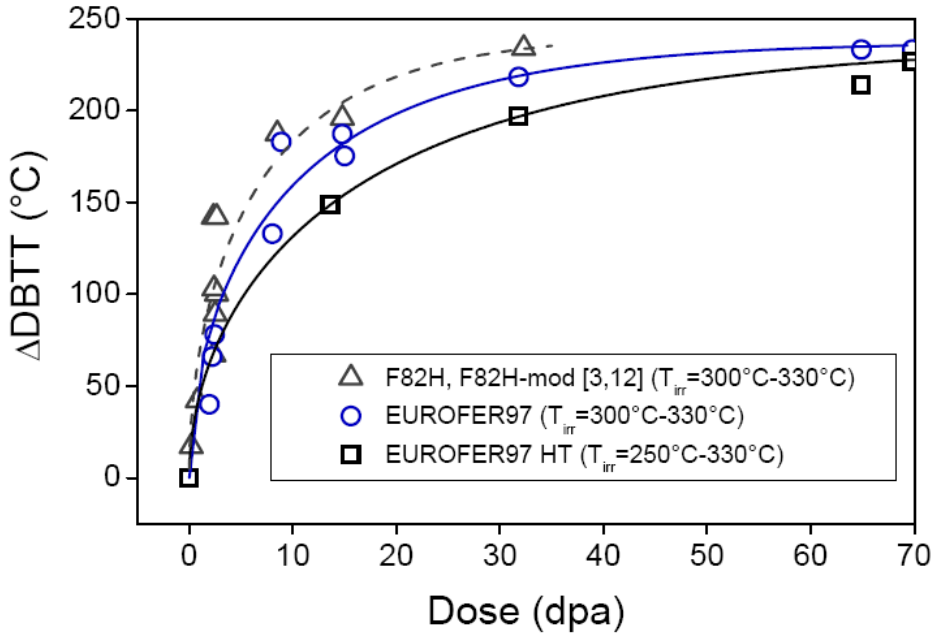

Fig. 4.6: Irradiation induced shift of DBTT for ferritic-martensitic steels F82H and EUROFER97

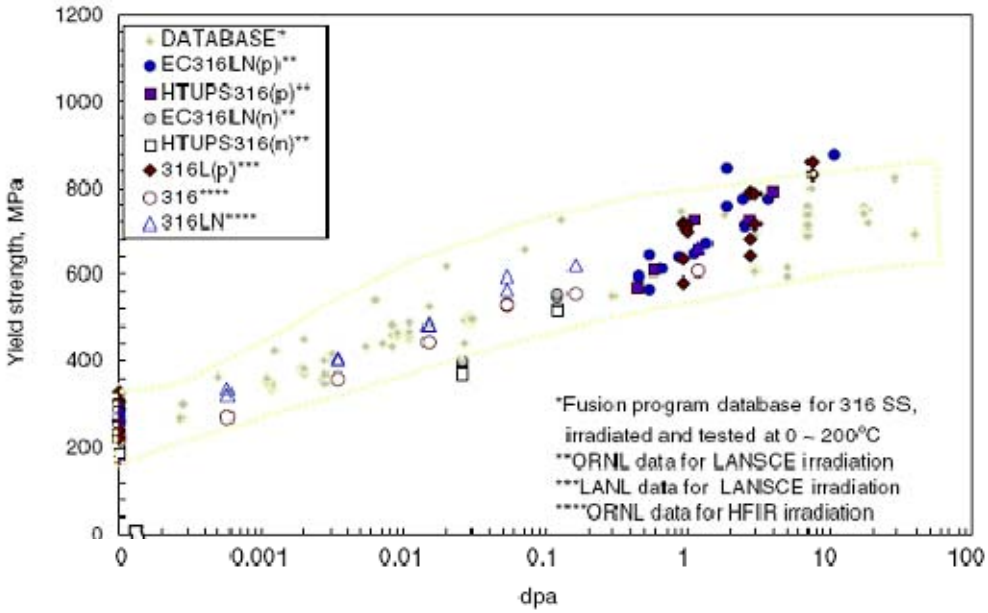

Fig. 4.7: Yield strength increase with dose for 316SS irradiated and tested in the temperature range of 0-200°C under spallation conditions [Mans06]

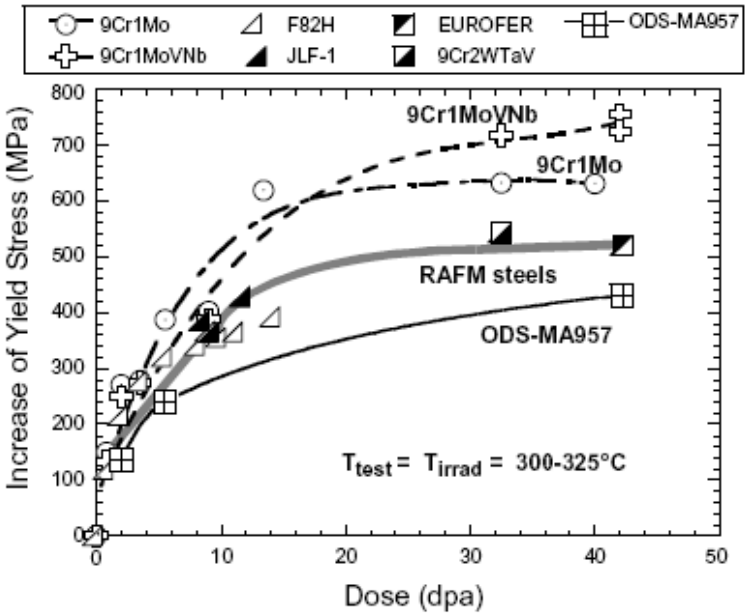

Fig. 4.8: Increase of yield strength for ferritic-martensitic steels (including EUROFER97) irradiated at 300-325°C up to 42 dpa [Alam07]

Swelling

Fig. 4.9 shows that swelling of RAFM is significantly lower than for 316L and 316L stabilized with titanium. Swelling of 316L-Ti at about 130 dpa is in the range of 6-9%, while it is below 1% even at 160 dpa for all tested RAFM.

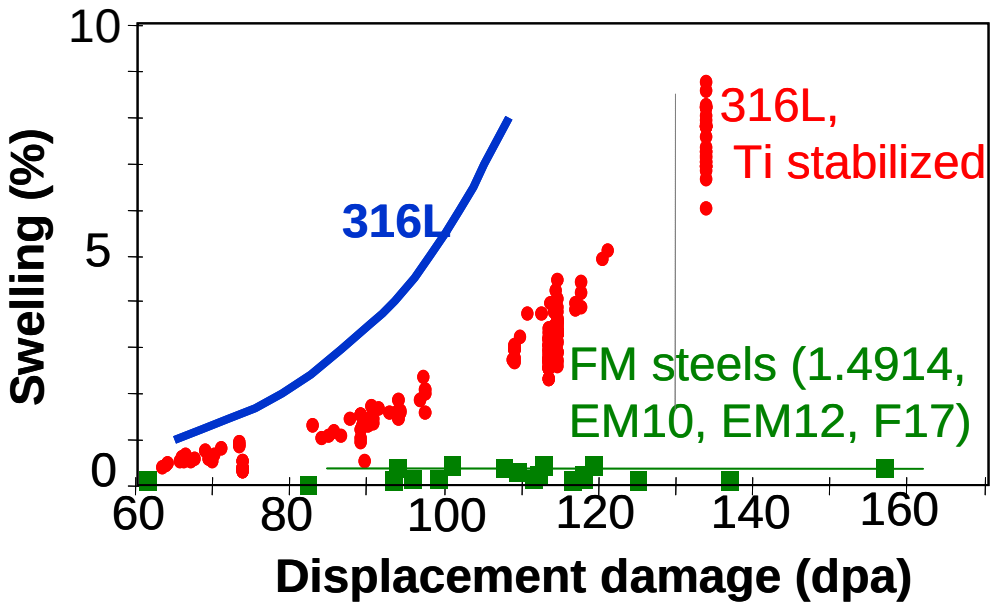

Fig. 4.9: Fuel Element Cladding irradiation in Phénix reactor

Hydrogen retention

High hydrogen production rate usually is not considered as a dangerous factor due to its high mobility. It can be however trapped by irradiation induced defects like voids and dislocation loops or at the surface of cracks. Retention of hydrogen increases brittleness of material and stimulates microcrack growth under fatigue conditions.

Helium accumulation

Helium is much less mobile than hydrogen in structural materials and can be trapped by vacancies, dislocations and grain boundaries. In the considered operation temperature range helium is assumed to be trapped mainly by radiation induced defects of small precipitates in the matrix body. For instance, the accumulation of 500 appm He under neutron at 420°C result in moderate hardening (60-100 MPa), slight increase of DBTT (25°C) and significant fatigue lifetime reduction (factor of 5) [Lind94, Osch00,Mate00].

References

[Zink00] S.J. Zinkle, N.M. Ghoniem, *Operating temperature windows for fusion reactor structural materials*, Fus. Eng. and Design **51–52** (2000) 55–71

[Robe97] J.P. Robertson, I. Ioka, A.F. Rowcliffe, M.L. Grossbeck and S. Jitsukawa, *Temperature dependence of deformation behavior of type 316 stainless steel after low temperature neutron irradiation*, ASTM STP (1997) 1325

[Gaga08] E. Gaganidze, H.-C. Schneider, C. Petersen, J. Aktaa, A. Povstyanko, V. Prokhorov, R. Lindau, E. Materna-Morris, A. Möslang, E. Diegele, R. Lässer, B. van der Schaaf, E. Lucon, Proc. of 22st IAEA Fusion Energy Conference, 13-18 October 2008 Geneva, Switzerland; Paper FT/P2-1.

[Mans06] L.K. Mansur, J.R. Haines, JNM 356 (2006) 1–15

[Alam07] A. Alamo et al., JNM 367–370 (2007) 54–59

[Lind94] R. Lindau and A. Möslang, J. Nucl. Mater **212-215** (1994) 599

[Osch00] E.V. van der Osch, M.G. Horsten, G.E. Lucas, G.R. Odette, in: M.L. Hamilton, A.S. Kumar, S.T. Rosinski, M.L. Grossbeck (Eds.), Effects of Irradiation on Materials, 19th internat. Symposium, ASTM STP 1366, American Society for testing and materials, West Conshohocken, PA, 2000, p. 612.

[Mate00] E.I. Materna-Morris, M. Rieth, K. Ehrlich; Effects of Irradiation on Materials, 19th internat. Symposium, ASTM STP 1366, American Society for testing and materials, West Conshohocken, PA, 2000, p.597

5 Criteria evaluation

5.1 Criteria associated with Performance during operation

This section describes criteria associated with performance during operation. The performance of the target at nominal conditions is essentially determined by the safety analysis measures and there in particular by the probabilistic safety assessment (PSA) for the design basis events The result of the PSA is the failure rate of the entire system for all conditions, in which no unacceptably large radioactive excess to the ambient (source term) is obtained.

It is clear that the operational instrumentation off the target as well as its detection devices essentially determine this availability. The instrumentation and detection monitors in the target must meet:

- the temporal behaviour of the target system, which means the detection of events before a degradation is obtained.
- The high flux in the active region. Thus they must have robust, well proven design with a high availability.
- Redundancy aspects. Potential target failure initiating events must be acquirable by different independent systems to start safety countermeasures.

The subsequent figure illustrates the main instrumentations foreseen to be implemented in the active part of the envisaged ESS target station.

The objective and type of instrumentation in the different target domains is subsequently described. First the sensors intended to instrument the liquid metal part of the target:

a.) The flow rate recording necessary to ensure an adequate target cooling and to establish a planar target liquid metal surface is conducted by using three different measures as thermocouples, pressure sensors and an electro-magnetic frequency flow meter. The temporal resolution of the flow meters demands due to the beam pulse repetition frequency of 20ms (50Hz) the thermocouples being small enough to be faster than these repetition frequency. This requires 0.5mm outer diameter sheeted thermocouples. By the heat balance the flow rate can be recalculated using the data acquisition system (DAQ). A measurement technique also non intrusively measuring directly the flow rate with an even larger temporal resolution is the electro-magnetic frequency flow meter (EMFM), see Schulenberg and Stieglitz (NED, 2009, [8]). Thermocouples have shown the capability to withstand long term irradiation conditions and hence can be conceived as reliable. The EMFM shown in figure 2 is consisting of three coils of which two are AC current fed. Since the EMFM is not intrusively measuring the flow rate by two different principles (RMS-Amplitude and phase-shift), the absence of moving parts and a liquid metal sensor contact it can be considered to be available at least to the same reliability as thermocouples. Regarding, pressure sensors, inductive and piezo-resistive versions show an excellent accuracy and temporal resolution, however, they do not exhibit a reliable irradiation resistance. Therefore, capacitive systems taking advantage of the relative movement of the membrane as they are used in NPP represent currently the most reliable sensor type. The temporal resolution is with 5 Hz relatively slow, but they simultaneously offer the capability to control the proper functioning of the pump system.

b.) Regarding the level metering four different principles are used. For the measurement of the liquid metal level in the container and the flow conditioner a simple electrode is used to detect if liquid is lost by a leak in the container or the target feed channel is not

fully filled to allow a target operation. The electrode provides a simple binary signal to be evaluated in the programmable logic controller (PLL) of the target safety system. A similar functional principle has the thermocouple T* indicated in figure 1. It is an open thermocouple providing by an electric short circuit of the two branches an indication of a perfect filling of the target flow conditioner. The level sensors used for the target container and the flow conditioner are identical. Regarding the monitoring of the free surface also a contact principle for the in pile operation is foreseen which corresponds to the one developed for the 10MW IFMIF irradiation target, see detail in [9]. It is depicted in figure 3 and capable to measure the surface position with a high degree of reliability. With respect to the V&V-phase (Verfication and Validation) more sophisticated must be used to quantify potential free surface flow instabilities arising from a nozzle degradation or pump defect , etc.. However, with respect to this in the context of the development of the Spallation targets for ADS within the EU-IP Eurotrans as well as in the EU fusion Braoder approach program such measures has been developed and validated for free surface liquid metal flows as reported in detail in the corresponding deliverables or in [9, 10]. The level metering in the target container hosting the liquid is complementary acquired by measuring the pressure of the liquid height in the container. In case of PbBi a height of 0.5 meters already delivers due its density a pressure difference of 0.5 bars.

c.) The temperature control in the liquid metal is conducted using conventional Ni-NiCr thermocouples operating up to 1200^{o}C, which is still 400K below PbBi boiling temperature. Since for a full power operation the mean temperature rise per pulse in the liquid will at nominal conditions not esceed 50K they can be expected to run for a longer time if even a loss of heat sink occurs.

d.) The pressure sensors are used to control both level height in the container as well as the pump functioning. As described here capacitive sensors seem to be most promising due to their robustness although they exhibit a low temporal resolution. However, since the liquid metal target operates as a low pressure target, the liquid turn around times in the target are much longer than the pulse repetition frequency of the beam. Due to the functional principle of the free surface target by a decoupling the pressure waves generated by the volumetric liquid expansion caused by the beam in using a free surface the inertia of the sensor does not affect the performance of the target unit.

Instrumentation in the secondary coolant liquid (water/steam):

a.) In the coolant water the feed water temperature as well as the excess water temperature is controlled using thermocouples. The temperature describes together feed water flow and with the pressure level set in the external steam condenser the removable thermal power from the target.

b.) The flow rate of the feed water as well as the excess water can be measured far outside the active region and is required to conduct a reliable heat balance and to the discovery of leaks.

c.) Similar to the flow meters the pressure sensors for the feed water as well as the steam line can be located outside the active target domain and hence conventional technology known from NPP can be used.

d.) In the excess water an activity meter should be placed. An enhanced activity exhibits if one of the steam tubes has potentially failed. From the safety aspect of the steam generator/cooler which will be designed according to the leak before break principle of a NPP this is not a functional deficit because the temperatures in the SG are

considerably below the melting point of the PbBi. Together with the high surface tension of PbBi in any small scale PbBi will rapidly solidify. However, if so still aquatic soluable active portions are dissolved in the excess water and allow an early stage failure detection.

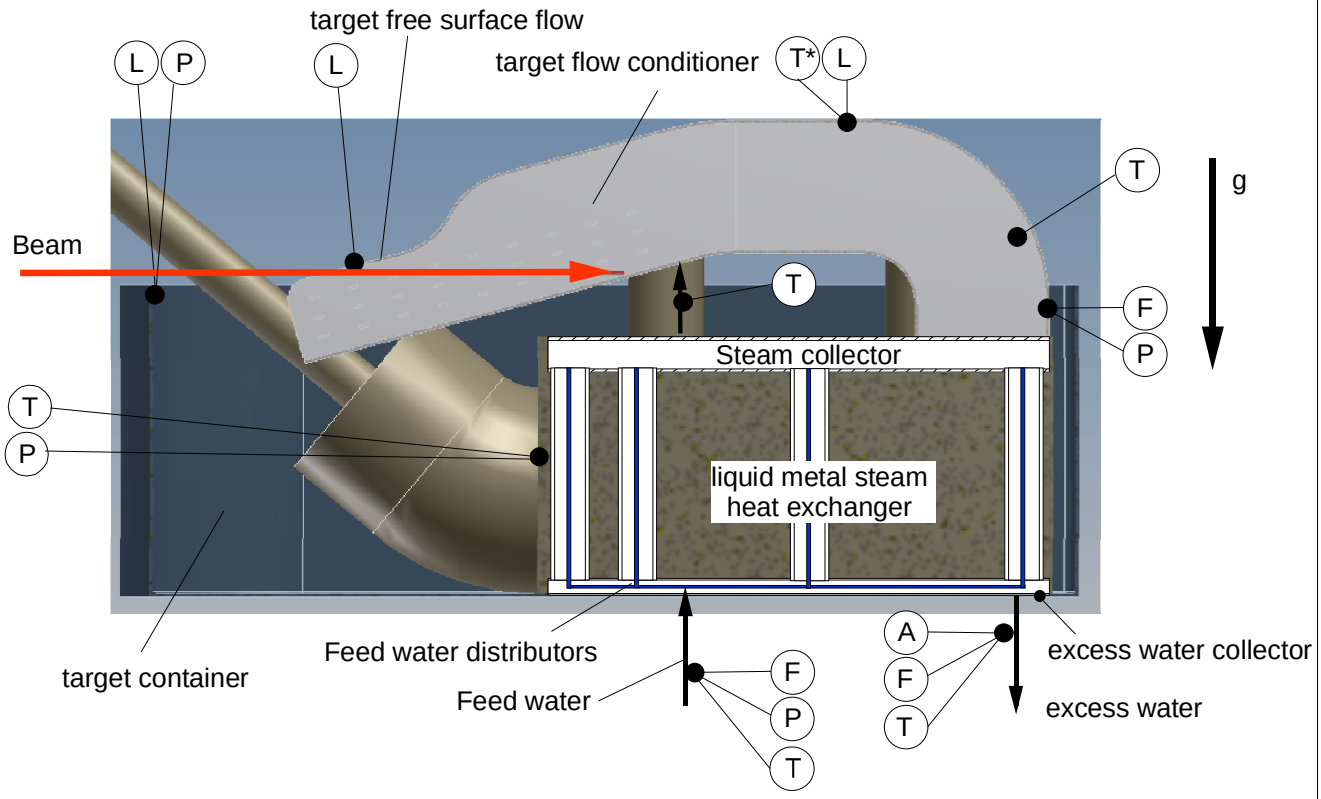

Fig. 5.1: Sketched of the instrumentation types and location required to control the liquid metal free surface target. The abbreviations denote : F=flow meter, P= pressure sensor, T= temperature, L = level meter.

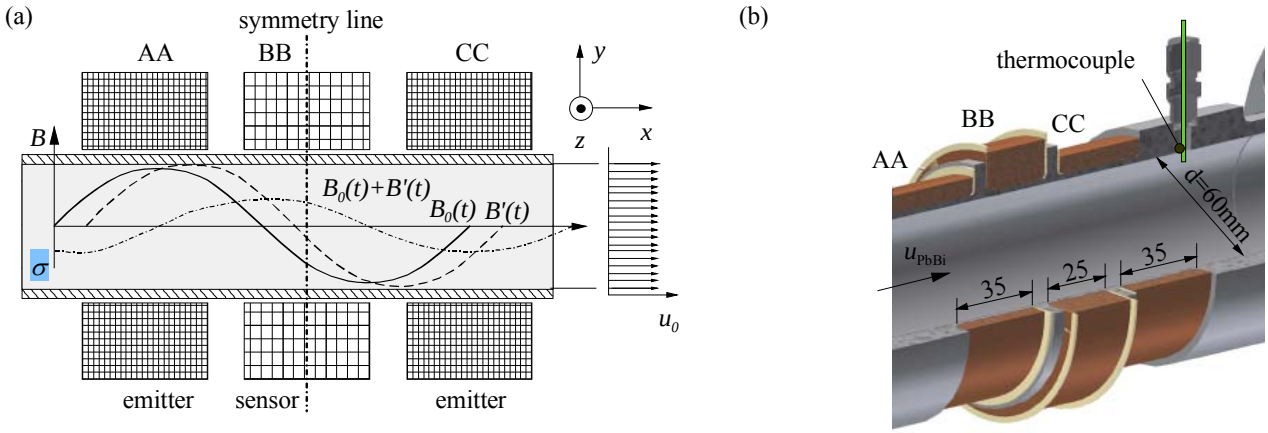

Fig 5.2: Function principle of an EMFM according to [8].

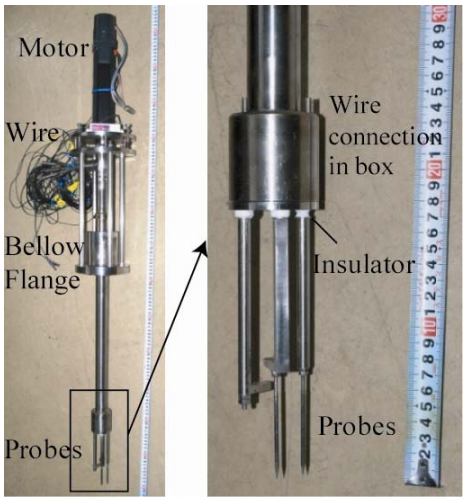

Fig. 5.3: Intrusive contact resistance probes developed for a high irradiation in the context of IFMIF by Horiike et al. (2009, [9]).

5.1.1 Neutron performance - Time Integrated flux instruments (SANS)

Evaluation…

5.1.2 Number of possible beam lines

Evaluation…

5.2 Criteria associated with Safety

This section describes criteria associated with performance during operation:

General guide lines and pre-requisites for commissioning a nuclear target

The design of the ESS target module has to match the international safety standards, the national standard acts and the subordinated local regulation authorities from the general guidelines in a way similar to nuclear power plant (NPP), however, on a more simplified level. Nevertheless, as all IAEA signed countries the operator is pledged to adequately protect the public, the professionals and the environment against the hazards of a radioactivity release. In this regulation the operator (constructor) has to proof the safety of the installation and of the operation during the entire lifetime cycle of the nuclear component to be commissioned. According to [7] this measure scopes the operation, the commissioning, the operation, the decommissioning and the disposal. In these general guidelines the operator provides the verification required that the implemented protection measures and functions correspond to the current state of the art in science and technology.

As mentioned the restrictions for a nuclear target deployment are considerably lower than for a NPP, but the target has to ensure for all probable design basis scenarios postulated to occur in the component as well as off-site events (arising e.g. by the accelerator, the operational stuff, off-site power loss, etc.) affecting the component the avoidance of unacceptably large radioactive source terms to the ambient. Therefore, any target design necessitates with respect to a safe operation a deterministic safety analysis and for its overall availability to the user a probabilistic safety analysis (PSA).

The general guidelines to be considered for design basis accidental (DBA) analysis scope all potential operational stages of the target and thus also the nominal operation. For the DBA analysis accidents are postulated to which the nuclear component must be designed to withstand the loads during likely occurring events without releasing harmful amounts of radioactivity. In DBA situations the safety and instrumentation systems has to monitor to set the countermeasures in such a manner that insignificant off-site consequences occur. In case of the liquid metal target these internal scenarios are:

- The filling procedure and the start-up sequence,
- The nominal operation.
- The shut-down sequence.
- The loss of heat sink and external cooling supply.
- Trip of the liquid metal pump.
- Leak of the target container.

Off-Site scenarios leading to a DBA are

- Unprotected beam focussing, beam trips, irregular beam repetition.
- Loss of off-site power
- Earthquakes or other scenarios likely to occur on-site to be specified by the regulating authority.

The outcome of this safety analysis is the safety demonstration of the component in the different operational stages and the quantification of the safety margins. Another output of the DBA analysis is the flexibility of the design in the different operational regimes in terms and hence allows to reliably conclude on an increased target cycle length or a power up-rating.

Once the potential initiating events are specified the DBA safety analysis can be conducted using a deterministic approach. This relies on most cases on mechanistic codes representing the mathematical/physical model of the target installation in which thermal-hydraulic (TH), neutron-kinetic (NK) and structural mechanics (SM) aspects are taken into account by using state of the art knowledge. The aim is to predict the response of the target installation to the postulated initiating events (PIE). It must be clearly stated that with respect to TH, NK or SM some components may exhibit considerable margins, however, non-linear component interactions, instrumentation limitations, different inertial frames may rapidly minimized the potential of a target concept. Therefore, without a credible DBA safety analysis the reliable prediction of an enhanced cycle length or an up-rating is of illusionary nature.

General assessment of the safety of the overall configuration

Prior to any dedicated safety and procedure measures the operation principle in view of the safety philosophy should be mentioned.

The principal design of the PbBi free surface target follows the idea of a low pressure unit allowing a multiple beam shot failure without taking any countermeasures either from the PLC or the operational staff. The general features are:

- low mean temperatures of the target material it self at simultaneously low temperature oscillations of any structural material.
- Low content of structural material in the most active region to minimize the amount of decommissionable waste.

- Low pressure in all components to prevent in case of severe accidents fast countermeasures in terms of pressure wave propagation with activated products.
- Minimization of activated media transport through auxiliary systems located outside the target container, as e.g. coolant lines, drain containers.
- Modular design (exchangeable pump, and nozzle section) reducing the preparation times for active target restarting. Replacement of target possible without renewal of the remaining target section.
- Redundancy of the target monitoring instruments by using physically different principles and well proven mostly nuclear validated principles.
- Simple and robust structure with low flow velocities and reduced recirculating or detached flows to minimize liquid metal corrosion and erosion and hence to limit the potential of stress or erosion initiated cracking or failure modes. All measures lead to a potentially large life time exceeding the envisaged values.
- Minimization of active components in the highly irradiated active domain. There are no rotating functional mechanical parts within the beam region, which may fail due to embrittlement or swelling. The only relative moving part is a floating bearing using the liquid itself as lubricant.

Principal safety assessment of the components

The liquid metal free surface target design consists essentially of three major components:

- The target container hosting the PbBi liquid storage tank and the PbBi-steam heat exchanger;
- The impeller pump driven via a gear mechanism from outside by an electro-motor and
- the target flow conditioner

All the components are individually fabricated and can be mounted together without any mechanical cut or welding procedure.

Subsequently the main features of the individual components are discussed.

a.) main target container the main target container the main target container contains of a vessel in which the PbBi-steam heat exchanger, the guide tube for the impeller pump and the vanes and sliding system for positioning the target flow conditioning system including the target is installed. Within this container the entire liquid of the loop system is installed. For the start-up the pump thrusts the fluid towards the target flow conditioner into the target station. The container is volumetrically designed in such a manner to provide a liquid level in the cold stand by that the impeller driven pump has a sufficient liquid level so that even at pump impeller speeds (PbBi-flow rates) considerably higher than at nominal conditions the liquid layer above the top of the impeller provides enough height to prevent cavitation within the impeller-wings. Fixed installed in the cavity is the PbBi-steam heat exchanger which requires four connections (if possible three) to the ambient supply system. One is for the feed water supplied by the water pump und one for the excess water; the other two provide the steam tubes directed towards the condenser. All can be attached using NPP reactor certified standardized tube fittings and sealings, which later simplifies the decommissioning considerably. Due to the relatively small pressures required for the pump (less than 2 bars) to attain the intended flow rate the container thickness likely to be fabricated of stainless steel remains at a reasonable weight and no specific welding procedures have to be applied. The container is not foreseen to be drained during a

replacement and serves still as the reservoir for the PbBi during its whole life time. Due to the excellent soluability of the Polonium in eutectic lead-Bismuth (PbBi), which is likely built up during operation, such a measure ensures containg the Polonium in a well defined environment. Such a philosophy implies that the container has to operation modes a cold standby during its life time and for the final decommissioning and disposal a defined freezing sequence for the liquid. All the instrumentation for the container is fixed installed

b. The impeller pump and gear drive mechanism can be installed even into the filled target container in case of a destruction. It is shifted from the side and top into the cavity of its guiding tube. In order to prevent a irradiation destruction of the electro-motor driving the impeller system a 90^{o} gear drive system is used, which allows a placement of the electro-motor outside the moderator regions. The transmission can be achieved using a temperature compensated cardan shaft. All its operational parameter relevant for the operational regulation can therefore installed outside without loosing any information.

c. Target flow conditioner and target (TFC). The TFC is likely experiencing the highest dose rates and fluxes and is the most essential part of the target. Due to these conditions the highest damage rates and hence the shortest life time can be expected. Therefore, the TFC is readily fabricated and instrumented and can be shifted by vanes into the target container, in which it is then axially fixed. Due to the low pressure conditions of the target the requirements for the sealing of the TFC to the target container are negligibly small and currently a press fitting without sealing seems more than feasible.

According to the general functional description of the individual units a simplified target flow sketch can be elaborated, which is shown in figure 4.

Before the discussion of the potential safety performance the potential of the most essential components should be briefly discussed.

Target flow conditioner and target (TFC):

a.) within the TFC the flow rate at nominal flow conditions remains in all target domains with wall contact considerably below 2m/s and hence neither corrosion nor erosion can be expected for years even using stainless steel as structural material. This holds especially for the nozzle forming the free surface flow, which experiences the highest wall shear stress.

b.) Free surface flow area designed exceeds the beam dimensions by about 25% in spanwise direction to allow also a beam misalignment. In order not to loose a too large flow rate fraction guide vanes as pressure drop obstacles are introduced below the liquid surface reduce the flow demands for the pump further.

c.) The free surface generating nozzle corresponds in its design to the FAIR AC beam operated target design. The flow behaviour dependent on the design can be numerically computed. The corresponding computational fluid dynamic models necessary to describe the flow as well as their validity ranges have been verified and experimentally proven at prototypical conditions including surface instability thresholds [11,12]. Using these tools the shape can be optimized for future upgrades further, since the limits for code and materials are by for not attained currently.

The pump necessary to drive the liquid through the heat exchanger and the TFC is an impeller pump using a similar design as in the XT-ADS reactor application, however, drastically downscaled. The design of the wing geometry will be in such a manner, that the

maximum velocity at the wing is below half of the critical flow rate for pump material erosion of 20m/s.

PbBi-Steam heat exchanger. Evaporation or steam coolers provide heat transfer coefficients far beyond forced convection coolers, due to the relatively large evaporation enthalpy of water Δh_v is at nominal pressure (1013 mbar) 2257kJ/kg in principal at a nominal power of the target of 5MW a water flow rate of 2.21kg/s (or $8m^3$/hr) only is required. However as computations [13] have shown, the dynamics of instantaneous evaporation somehow by factor two larger water flow rates are required. Nevertheless, evaporation coolers offer a unique capability. Both by an increased water flow rate and by a reduction of the steam condenser pressure the power removal capability can be considerably improved without any design changes. This allows a simple fine regulation of the thermal power removal. Additionally, they exhibit excellent safety features. Due to the low pressure inside the steam tubes no thick walls are required. In case of a steam tube leak the steam temperature remains at all operation conditions below the melting point of PbBi. Applying NPP design rules ensuring a leak before break accidental scenario a freezing of the PbBi in the leak can be easily ensured. This holds even for the case of failure of the depresserization pump setting the steam pressure, at 1bar only 100°C can be attained. An other positive feature of the evaporation cooler is that the coolant liquid volume being irradiated (which is at the end of life waste) is minimal compared to a forced convection coolant systems. Not used water is drained by gravity in the excess line. The evaporation cooler allows also a fast response in case of a beam loss. Then the water feed is interrupted and the remaining water in the cooler is evaporated to the steam line. In a short time no water is present in the heat exchanger (HEX). On the other hand due to the minor quantity of the water stored in the evaporators the amount located in the HEX is not sufficient at any time to freeze the liquid metal.

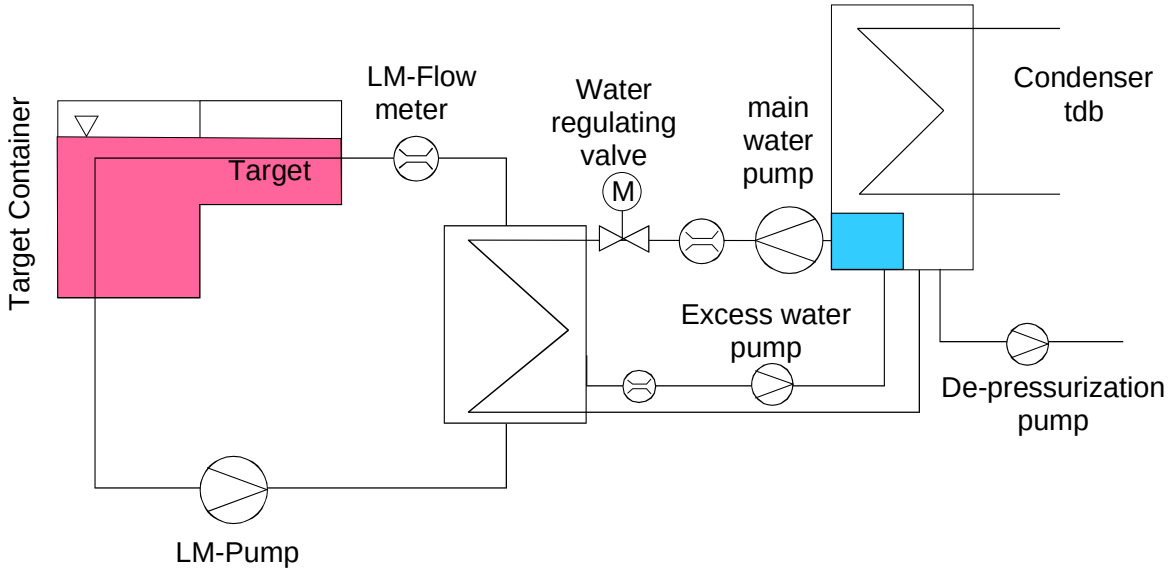

Fig. 5.4: Simplified flow sketch of the for the free surface liquid metal ESS target proposal by KIT.

Potential DBA scenarios of the KIT free surface target and responses

A full deterministic model of a DBA analysis for the KIT target has not been conducted up to now. However, the detection mechanisms as well as the corresponding time scales and necessary countermeasure can be defined and roughly assessed.

<u>The unprotected loss of heat sink and external cooling supply (ULOHS).</u>

Event initiator:

The LOHS can occur either by a failure of the main water pump or an undetected steam tube break within the heat exchanger which is large enough to close the feed water line. This should be detected by flow meter in the water system or the activity meter in the feed water excess line. In case both fail the target temperature rises. Since the target is designed to attain at maximum a temperature rise of 50K per shot about 10 full power shots are still possible assuming no recording of the thermocouples to disconnect the beam. The target still remains its integrity without loosing its performance or. This corresponds to a time of about 0.5seconds. Then however the temperature of the back-wall reaches about 650^{o}C where the maximum allowable yield strength rapidly degrades. Nevertheless, the target is still not entirely damaged and likely only the TFC needs to exchanged.

Trip of the liquid metal pump.

A failure of the pump immediately yields to a drain of the target system. Due to the inertia of the liquid metal in the loop and the volume up the nozzle exit a film can likely be maintained over a tenth of a second probably a little more preventing a total distruction. Nevertheless, a pump trip demands a rapid detection and hence a fast data acquisition system recording shaft rotation speed, temperatures and pressure.

Leak of the target container.

Aside from the radiological source term a leak of the target container does not lead to an immediate loss of the target performance and hence may allow a further target operation if it can be localized and stopped. The lower limits of the liquid metal level within the container can be recorded by the installed level meters in the TFC and the target container as well as the pressure gauge. In case the safety authority demands a second hull the design allows to accommodating for this request.

Literature

[7] IAEA-INSAG-12, Safety requirements for nuclear installations, weblink http://www.pub.iaea.org/...

[8] Th. Schulenberg, R. Stieglitz (2009), Flow measurement techniques in heavy liquid metals, Nuclear Eng. Desg., NED-5547.

[9] H. Horiike, T. Kanemura, H. Sugiura, N. Yamaoka, S. Suzuki, H. Kondo, M. Ida, M. Miyashita, H. Nakamura, K. Watanabe, 2009, Diagnostics and Instrumentation for a Lithium free surface target in IFMIF, Design review IFMIF/EVEDA on Diagnostics and Purification Systems, JAEA, Tokyo.

[10] M.P. Hillenbrand, R. Stieglitz, T. Schmidt, T. Schulenberg, 2008, Detection of liquid metal surfaces using the DLP measurement technique, Proc. 3rd Conf. Heavy liquid metal coolants in nuclear application, Obninsk, Russia.

[11] S. Gordeev , L. Stoppel ; R. Stieglitz, 2009, Turbulent liquid metal flow in rectangular shaped contraction nozzles for target applications, International Journal of Computational Fluid Dynamics, p.477-493

[12] S. Gordeev ,R. Stieglitz, V. Heinzel, 2010, LARGE EDDY SIMULATIONS OF TAYLOR-GÖRTLER INSTABILITIES IN TRANSITIONAL AND TURBULENT BOUNDARY LAYERS Proceedings of ASME 2010 3rd Joint US-European Fluids Engineering Summer Meeting and 8th International Conference on Nanochannels,

Microchannels and Minichannels FEDSM-ICNMM 2010 August 1-5, 2010, Montreal, Canada FEDSM-ICNMM2010-30267

[13] R. Stieglitz, U. Müller, 1995, *GEODYNAMO Eine Versuchsanlage zum Nachweis des homogenen Dynamoeffektes, FZKA-5718.*

5.2.1 Ease of containment implementation

Evaluation…

5.2.2 Environmental impact beyond design basis accidents

Evaluation…

5.2.3 Ease of licensing approval

Evaluation…

5.3 Criteria based on Associated Risks

5.3.1 The need for R&D

Evaluation…

5.4 Criteria based on Availability

5.4.1 Lifetime of TMR

This evaluation should take into account irradiation damage sensitivity and liquid metal environment sensitivity.

Evaluation...

5.5 Criteria based on Maintainability

5.5.1 Time required to perform maintenance/service

Evaluation…

5.5.2 Ease of TMR exchange

Evaluation…

5.6 Criteria based on Upgradability

5.6.1 Possibility to increase performance of existing system

Evaluation...

6 Summary